



Machine learning and deep learning approaches for soil classification: methods, challenges, and future prospects

Kuldeep Pal & Nidhi Gupta

To cite this article: Kuldeep Pal & Nidhi Gupta (2025) Machine learning and deep learning approaches for soil classification: methods, challenges, and future prospects, International Journal of Remote Sensing, 46:22, 8488-8545, DOI: [10.1080/01431161.2025.2570552](https://doi.org/10.1080/01431161.2025.2570552)

To link to this article: <https://doi.org/10.1080/01431161.2025.2570552>



Published online: 16 Oct 2025.



Submit your article to this journal [↗](#)



Article views: 63



View related articles [↗](#)



View Crossmark data [↗](#)



Machine learning and deep learning approaches for soil classification: methods, challenges, and future prospects

Kuldeep Pal and Nidhi Gupta

Department of Computer Applications, National Institute of Technology, Kurukshetra, India

ABSTRACT

Classifying soil types is an essential for environmental monitoring, agriculture, and civil engineering. Conventional techniques for classifying soils frequently depend on laborious laboratory tests or arbitrary field evaluations, which can create unpredictability and irregularity. This paper examines new developments that combine deep learning and digital image processing for automated, quick, and repeatable soil categorization in order to get beyond these restrictions. The visually evident qualities of soil texture, color, and surface structure—all traditionally utilized by soil scientists for field identification—can be statistically examined by imaging techniques. Researchers have shown a strong correlation between image-based features and lab-tested soil properties like moisture, clay content, and organic matter by extracting spectral signatures and textural features (such as RGB, hyperspectral, and multispectral) from digital soil images and using models like convolutional neural networks (CNNs) and transfer learning. The current status of image-based soil classification research is critically reviewed in this article, with an emphasis on the field's scientific foundation, technical difficulties, and applications. The significance of collaboration among soil experts, the quality of the dataset, and the validation of the model using ground-truth soil lab results are all emphasized. The paper also describes how these models could be used in the field in real time to promote sustainable land use and precision agriculture. Our results imply that image-based deep learning offers a useful supplementary strategy to improve the speed and objectivity of soil classification when appropriately established in soil science and verified using traditional techniques.

ARTICLE HISTORY

Received 7 May 2025

Accepted 28 September 2025

KEYWORDS

Hyperspectral image;
multispectral image;
convolutional neural
networks

1. Introduction

Soil is a fundamental natural resource that underpins agricultural productivity, environmental sustainability, land use planning, and ecosystem health. Its properties including organic matter content, texture, structure, and colour determine crop suitability and influence water retention, nutrient availability, and plant growth dynamics (Hemdan and Al-Atroush 2024). Global classification systems, such as the Food and Agriculture Organization's world reference base and the United States Department of Agriculture's

(USDA) taxonomy, provide standardized methods for categorizing soils, thereby facilitating research and practical applications across multiple domains (Gyasi and Purushotham 2023).

With the world's population projected to exceed 9 billion by mid-century, the demand for food continues to place unprecedented pressure on agricultural systems. Effective crop production requires selecting suitable soil types, as different soils vary in water-holding capacity and fertility. For example, sandy soils drain rapidly and often demand frequent irrigation, while clay-rich soils retain water but pose challenges for aeration (Uddin and Hassan 2022). Consequently, soil classification plays a pivotal role in optimizing land use and ensuring food security (Carlomagno et al. 2024). However, traditional classification methods – based on labour-intensive physical and chemical analyses – are often costly, time-consuming, and unsuitable for large-scale applications (Ahmad 2023; C.-Y. Liu et al. 2024). In recent years, digital and computational approaches have transformed soil assessment methods such as geographic information systems (GIS) and remote sensing have enabled large-scale mapping of soil characteristics by integrating terrain, climate, and soil datasets. As Sarkar et al. (2018) applied binary logistic regression and artificial neural networks to predict soil erosion susceptibility in Purulia district, West Bengal, India, producing validated susceptibility maps that support land-use planning, soil conservation, and agricultural management (Sarkar and Mishra 2018). Similarly, Rahman et al. (2023) developed a GIS-based framework that combined satellite-derived digital elevation models (DEM) with soil physical properties to generate land suitability maps for combine harvester operations in Bangladesh, thereby improving mechanized farming efficiency and resource allocation (Rahman et al. 2023). These advancements illustrate the potential of combining spatial data with computational techniques to improve soil resource management.

Parallel to GIS, advances in artificial intelligence (AI) and image processing technologies have opened new avenues for soil classification. Image-based techniques leverage visual data to analyse and classify soil types, providing a faster and often more accurate alternative to conventional methods (Kiran Pandiri, Murugan, and Goel 2024). This shift towards computer-based classification systems is particularly relevant given the increasing availability of high-quality imaging devices, such as digital cameras and smartphones, which enable the collection of rich visual data in diverse agricultural settings (Tobiszewski and Vakh 2023). Machine learning (ML) and deep learning (DL) algorithms, particularly convolutional neural networks (CNNs), have proven highly effective in identifying complex soil patterns by automatically extracting features from images and integrating ML and DL into image-based soil classification represents a significant advancement in this field. ML algorithms, which can identify patterns and make predictions based on data, have been successfully applied to various agricultural challenges, including soil classification (Kim et al. 2024). These algorithms can analyse large datasets and improve their performance over time, making them well-suited for the complexities of soil variability (Bouslihim, Rochdi, and Paaza 2021). DL, a branch of machine learning that utilizes multilayered neural networks, has significantly advanced the effectiveness of image-based classification. CNNs are highly effective in analysing visual data, enabling automatic feature extraction from soil images and minimizing the dependency on manual feature engineering (LeCun et al. 1998). In CNN, the input data undergoes convolution with filters in the intermediate layers, producing feature maps. Each feature map corresponds to a specific level of abstraction, which is determined by the softmax algorithm. In some cases, deep learning techniques are combined with

traditional image processing methods to enhance accuracy, as shown in [Figure 1](#). For example, statistical measures are used to analyse colour, texture, and shape, and classification is performed using a support vector machine (SVM) (Srunitha and Padmavathi 2016).

As the agricultural sector faces the dual challenges of increasing productivity and sustainability, innovative solutions such as image-based soil classification are essential. By leveraging the capabilities of machine learning and deep learning, scholars and professionals can develop more efficient, accurate, and scalable methods for understanding soil dynamics, ultimately contributing to enhanced food security and sustainable agricultural practices.

The primary objectives of this study are as follows.

- (1) To review and analyse the integration of deep learning and digital image processing in soil classification, assessing their accuracy, efficiency, and potential to replace or complement traditional laboratory and field methods.
- (2) To identify the scientific principles, technical challenges, and practical applications of image-based soil classification, emphasizing its role in enhancing sustainability, precision agriculture, and real-time field deployment.
- (3) To examine the role of hyperspectral and other remote sensing imaging techniques in advancing automated soil classification, with an emphasis on deep learning approaches, spectral feature extraction, and their applications in environmental monitoring and precision agriculture.

In this study, A unique perspective has been introduced that addresses previously unexplored aspects of the subject matter:

- (1) A systematic review of previous research on soil classification and analysis was carried out following the PRISMA guidelines 2020.
- (2) Analyse the state of the image-based soil classification by exploring the application of machine learning and deep learning models alongside image processing techniques utilized in various studies.
- (3) Identify and discuss the strengths and limitations of different methodologies employed in image-based soil classification to provide a comprehensive understanding of their effectiveness.

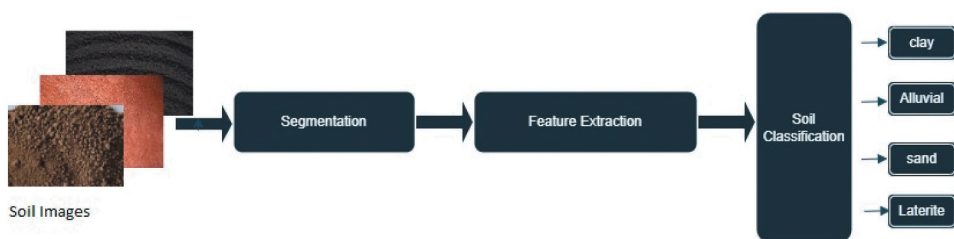


Figure 1. Digital image processing cycle.

- (4) Evaluate the implications of these technologies on agricultural practices, focusing on their potential to enhance soil management strategies and improve crop productivity.

The structure of this research paper is divided into eleven sections as follows: [Section 2](#) explains the basics of imaging techniques; it covers the properties of soil via laboratory test, including its composition, texture, colour variations, and physical characteristics. [Section 3](#) outlines the systematic approach taken to review and analyse existing literature. [Section 4](#) gives an overview of scientometric analyses, research trends, impact, and collaborations using quantitative methods, aiding in the evaluation and evolution of scientific knowledge with the help of tools like VOSviewer. [Section 5](#) gives an overview of publicly available and research-based soil image datasets. [Section 6](#) presents various soil classification methods utilizing image processing and computer vision. [Section 7](#) delves into advanced computational techniques for soil classification as ML and DL. [Section 8](#) contains a detailed discussion of different metrics used to assess the efficiency of the soil categorization framework. [Section 9](#) summarizes the key insights from the review, emphasizing major findings and contributions. [Section 10](#) highlights existing challenges in soil classification methodologies. [Section 11](#) suggests potential areas for further research and advancements in soil classification techniques, including improvements in dataset availability, model performance, and real-world applicability.

2. Imaging techniques

Classification of soil can be approached by examining various features, such as particle size (clods or aggregates), texture, and colour, either independently or in combination. Colour serves as a vital indicator of the physical characteristics and chemical composition of the soil, enabling researchers to extract significant statistical insights through colour analysis. Similarly, soil texture – primarily defined by the proportions of clay, silt, and sand – has been extensively utilized in methodologies to identify soil types accurately. The physical makeup of different soil types, including clay, loam, and sandy soils, allows them to have recognizable surface textures and colour characteristics. These features can be extracted using image processing techniques (such as histogram-oriented gradient descriptors, histogram features, or gabor filters), and DL models can pick up discriminative patterns to enable precise categorization. According to the de Oliveira Morais et al. [2019](#) after separating soil sections using image segmentation, features are extracted to capture patterns of colour, texture, and granularity. In order to forecast soil characteristics like clay and sand content, these image derived data are examined using multivariate approaches, such as partial least squares (PLS) regression. Imaging provides a high classification accuracy alternative that is quicker, less expensive, and more environmental friendly than conventional laboratory techniques. Recent advancements in digital imaging allow for rapid and non-destructive soil texture classification. In this approach, standardized digital images of soil samples are analysed to extract meaningful features, forming matrix **X**:

X = matrix of image features (e.g., texture, color, granularity), Size: $n \times p$

where n is the number of images and p is the number of features per image. Corresponding soil properties measured via laboratory tests (e.g. clay or sand content) are stored in vector \mathbf{Y} :

$$\mathbf{Y} = \text{targets oil property, Size: } n \times 1$$

PLS regression is applied to relate image data (\mathbf{X}) to soil properties (\mathbf{Y}) using the model:

$$\mathbf{Y} = \mathbf{X} \cdot \mathbf{B} + \boldsymbol{\varepsilon}$$

where \mathbf{B} is the matrix of regression coefficients and $\boldsymbol{\varepsilon}$ is the error term. For new images, predictions are made using:

$$\hat{\mathbf{Y}}_{\text{new}} = \mathbf{X}_{\text{new}} \cdot \mathbf{B}$$

This imaging-based technique offers a fast, cost-effective, and accurate alternative to traditional soil classification methods (de Oliveira Morais et al. 2019). Singh and Kasana, (2019) demonstrated that hyperspectral and multispectral imaging techniques capture both spatial and spectral information from soil samples. Each image is represented as a 3D data cube:

$$\mathbf{I}(x, y, \lambda) \in \mathbb{R}^{m \times n \times b}$$

where, x, y are spatial dimensions (image width and height), and λ represents the spectral bands (b) across different wavelengths. This image cube is reshaped into a 2D feature matrix:

$$\mathbf{X} \in \mathbb{R}^{N \times b}$$

where, $N = m \times n$, and each row represents the spectral signature of a pixel.

To reduce redundancy and noise, dimensionality reduction techniques such as principal component analysis (PCA) are applied:

$$\mathbf{X}_{\text{reduced}} = \mathbf{X} \cdot \mathbf{W}_{\text{PCA}}$$

where \mathbf{W}_{PCA} is the projection matrix containing the top k eigenvectors. The reduced feature set $\mathbf{X}_{\text{reduced}}$ is then input into ML or DL models like CNNs or long short-term memory (LSTMs) to predict target soil properties:

$$\hat{\mathbf{Y}} = f(\mathbf{X}_{\text{reduced}}; \mathbf{q})$$

where, f is the learned model and θ are the model parameters. The target vector $\mathbf{Y} \in \mathbb{R}^{N \times 1}$ may represent organic carbon content, clay percentage, or soil class label. Model accuracy is often improved through iterative training and validation. In a similar way, various scientists and researchers have done numerous research related to the soil classification (Singh and Kasana 2019).

Furthermore, recent studies have investigated the prediction of pH values as an additional means of characterizing and classifying soil. As a result, methods that emphasize the qualitative distinction of soils based on colour and texture have gained traction in the field. There is a notable increase in interest among researchers to develop automated processes for classifying soil images into spatial entities, thereby replacing traditional, labour-intensive manual procedures. In recent years, a variety of algorithms have emerged, leveraging both conventional image processing techniques and advanced computer vision approaches. By synthesizing current research, this paper seeks to shed light on the future potential of

automated soil classification technologies, ultimately contributing to more sustainable agricultural practices and environmental management. Moreover, texture is a key characteristic that reveals essential properties of soil images, reflecting the local statistical attributes of consistent or varying models. In the recent years, soil classification research has gained considerable attention, particularly in the study of textural characteristics.

3. Methodology used in literature review

The analysis was carried out to determine the best methods related to soil classification by using PRISMA guidelines, and research databases such as Scopus and Web of Science (Htun, Biehl, and Petkov 2023; Moher et al. 2009; Sujatha and Jaidhar 2024). Further, to identify relevant articles, we accessed Scopus and Web of Science research databases for the following questions as:

- (1) What are various approaches used for soil classification?
- (2) Which soil properties are most commonly used to classify soil types?
- (3) What are the different methods employed for collecting soil data?
- (4) What regions have been studied concerning soil classification?
- (5) How is the performance of classification models evaluated?

The technique utilized in this systematic review is illustrated in [Figure 2](#). It provides a clear visual representation of the systematic process of identifying, screening, and selecting relevant articles for a review or study, following the typical steps of a literature review methodology.

We followed a methodology to select the most relevant publications for this analysis. Initially, during identification, the following four queries were performed to search for the articles in the Scopus database:

- (1) TITLE-ABS-KEY (((‘soil classification’ OR ‘soil analysis’) AND (‘CNN’ OR ‘Convolutional Neural Network’) AND (‘image processing’)) OR ((‘soil classification’ OR ‘soil analysis’) AND (‘Machine learning’) AND (‘image processing’)))
- (2) TITLE-ABS-KEY (((‘soil classification’ OR ‘soil analysis’) AND (‘crop growth’) AND (‘image processing’)) OR ((‘soil classification’ OR ‘soil analysis’) AND (‘Deep Learning’ OR ‘CNN’ OR ‘ViT’ OR ‘multimodal’ OR ‘Multifusion’)))
- (3) TITLE-ABS-KEY (((‘soil classification’ OR ‘soil analysis’) AND (‘tillage’) AND (‘image processing’)) OR ((‘soil classification’ OR ‘soil analysis’) AND (‘Hyperspectral imaging’)))
- (4) TITLE-ABS-KEY (((‘soil classification’ OR ‘soil analysis’) AND (‘remote sensing’)) OR ((‘soil classification’ OR ‘soil analysis’) AND (‘Multispectral imaging’)) OR ((‘soil classification’ OR ‘soil analysis’) AND (‘soil texture’) AND (‘soil color’)))

To identify relevant research articles, queries are designed to filter studies based on the combination of approaches and soil properties mentioned. The terms included in the queries like soil paired with ML, multispectral, remote sensing, CNN, and image processing, etc., within the article’s content. Each query also targets specific keywords found in the title, abstract, or metadata. For example, Query 1 focuses on the studies related to soil

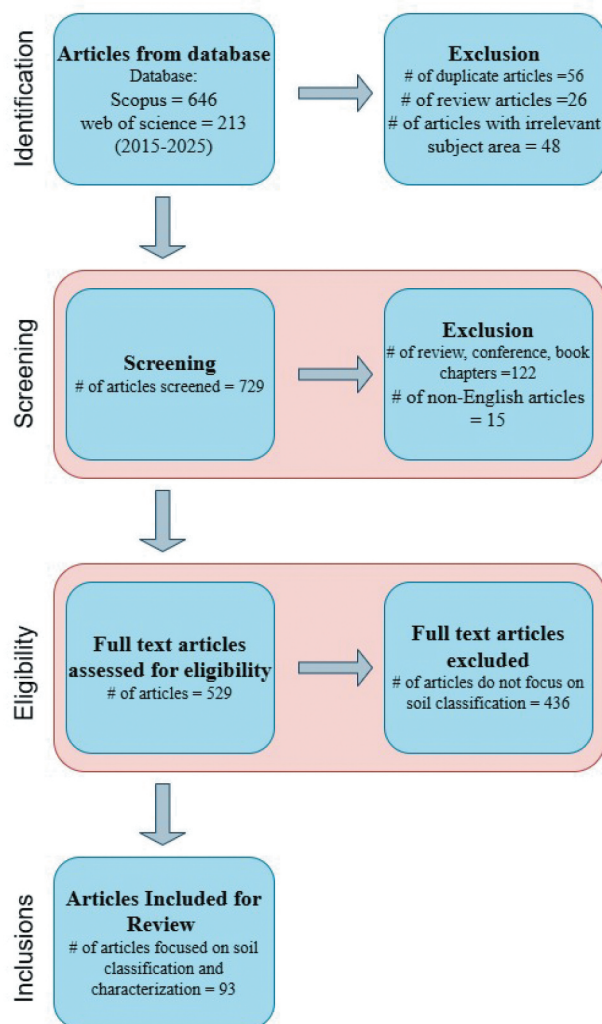


Figure 2. Methodology used in review process.

classification parameters. It looks for articles containing terms such as soil combined with classification or analysis and ML, CNN, and image processing in their title, abstract, or keywords. The aim of query 2 in this review paper is to identify research articles that focus on soil classification and analysis in the context of crop growth, utilizing advanced techniques such as image processing, DL, CNN, vision transformers (ViTs), multimodal approaches, or the multi-fusion method. This query seeks to gather studies that explore the intersection of soil classification and cutting-edge computational methods to enhance agricultural outcomes, particularly regarding crop growth and productivity. It highlights the integration of modern technologies like DL and multimodal frameworks for more accurate and efficient soil analysis. The aim of query 3 in this review paper is to identify research articles that investigate soil classification and analysis in the context of tillage

practices or the application of hyperspectral imaging. Specifically, it seeks studies that explore:

- The use of image processing techniques for soil classification and analysis related to tillage.
- The application of hyperspectral imaging for detailed soil analysis and classification.

The query focuses on integrating advanced imaging and analytical methods to enhance understanding and evaluation of soil properties, particularly in agricultural contexts involving tillage and precision soil analysis. The objective of Query 3 is to filter the articles to identify and synthesize research at the intersection of soil classification, tillage performance, and image processing techniques, with a particular emphasis on advanced methodologies like hyperspectral imaging. By including keywords such as 'soil classification', 'soil analysis', and 'tillage', the query focuses on studies that analyse soil properties and characteristics concerning agricultural tillage practice. The mention of 'image processing' highlights the interest in exploring how digital image analysis contributes to understanding soil texture, structure, and aggregate patterns. Additionally, the inclusion of 'hyperspectral imaging' expands the scope to advanced imaging technologies that capture soil characteristics across multiple spectral bands, enabling detailed composition, nutrient levels, and moisture content. Overall, the query reflects an interdisciplinary approach, bridging soil science, agricultural engineering, and image processing, to review existing research and highlight the role of image-based methods in sustainable agriculture.

Query 4 searches the publication for the review paper to identify and review research that explores the use of remote sensing and imaging technologies for soil classification and analysis, focusing specifically on soil texture and soil colour. By including keywords such as 'soil classification' and 'soil analysis', the query targets studies that examine various methods to understand and categorize soil properties. The addition of 'remote sensing' and 'multispectral imaging' highlights the intent to explore advanced technologies that enable large-scale and detailed analysis of soil features using spatial and spectral data. Furthermore, the inclusion of 'soil texture' and 'soil colour' suggests an interest in specific physical and visual attributes of soil that are critical for application in agriculture, land management, and environmental monitoring. This query demonstrates a comprehensive approach to identifying literature that combines traditional soil characterization with forefront imaging and sensing technologies to enhance soil assessment and classification practice. The execution of three queries yielded a total of 646 from Scopus and 213 articles from Web of Science, respectively, accumulating to 859 articles spanning from 2015 to 2025. After consolidating the results from these queries, 50 duplicate articles, 26 review articles, and 48 articles with irrelevant subject areas were identified and eliminated, and the articles associated with unrelated disciplines such as mathematics, economics, soil biology, and genetics were removed, leading to a refined total of 729. Then, these 729 articles were further analysed for the screening after excluding 122 conferences, and book chapter articles, as well as 15 non-English articles, the number of articles remaining was 592. Then, in eligibility, 592 full-text articles were assessed for eligibility, and 436 articles were excluded as they did not focus on soil

classification. Then, the total number of articles considered for review was 93, which focused on soil classification and characterization.

4. Bibliometric trends in soil classification

In conducting the systematic literature review (SLR), we aim to employ a robust methodology that combines critical review and scientometric analysis. This approach allows for a multifaceted examination of the research domain, drawing insights from both qualitative and quantitative perspectives (X. Zhao et al. 2020). Complementing the critical review, the scientometric analysis leverages various techniques to uncover patterns, trends, and connections within the research landscape. This may include bibliometric analysis to examine publication trends, citation networks, and collaborative relationships among researchers and institutions. Additionally, the network visualization can provide valuable insights into the global distribution of research activities and the influential roles of different countries or regions. In this approach to the SLR, we have carefully selected a set of freely available tools to facilitate the scientometric analysis component. This decision was informed by the recent work, which provides a comprehensive listing and categorization of such tools, including CiteSpace, BibExcel, HistCite, Publish or Perish, BibliTools (Python), and VOSviewer. After thorough consideration, we have chosen to utilize the VOSviewer software for our scientometric mapping efforts. This is widely recognized and versatile tool that enables the visualization and analysis of bibliometric networks. The selection of VOSviewer is based on its robust capabilities in handling and interpreting bibliometric data, as well as its user-friendly interface and extensive documentation (Li, Goerlandt, and Reniers 2021). This study employs scientometric analysis, incorporating various bibliometric techniques such as co-occurrence analysis (author keywords and all keywords), co-authorship analysis (authors), co-citation analysis (cited authors and references), and citation analysis by country. Some of the authors have provided detailed guidelines to utilize VOSviewer for analysis (Li, Goerlandt, and Reniers 2021; Van Eck and Waltman 2014).

Figure 3 depicts the connections and relationships between various countries. This type of analysis can be valuable in the context of SLR research paper, as it can help identify patterns and potential insights about the global landscape and the interdependencies among nations. The network shows that countries like China, India, and Russian Federation occupy central positions, suggesting their prominent roles and influence on the global stage. This could indicate their significance in the research domain or the broader context being explored in the SLR. The visualization reveals some geographical clustering, with countries in close proximity, such as the European nations to exhibiting stronger connections. Countries like Argentina, Serbia, and Morocco appear to have fewer direct connections, potentially indicating more isolated or specialized roles within the global landscape. This could highlight opportunities for these nations to explore new avenues for collaboration and diversify their international partnerships. By incorporating this type of network analysis into the SLR, researchers can gain valuable insights into the underlying pattern and dynamics of international collaboration, knowledge sharing, and the influence of different countries within the research domain. This information can be used to contextualize the findings, identify potential research gaps or opportunities, and informing strategic decision-making for future research direction.

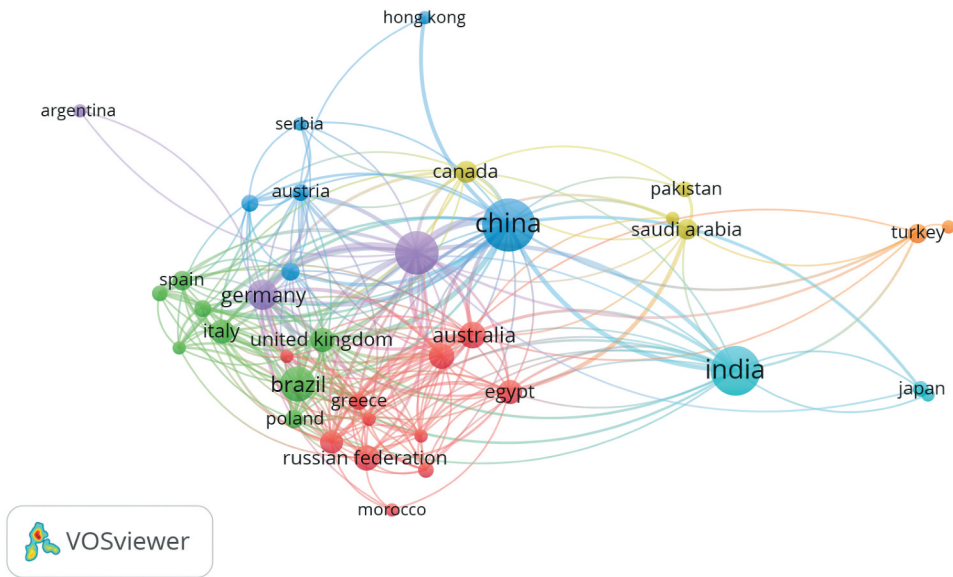


Figure 3. Co-authorship relations between countries.

Keywords networks can reveal trending topics and the overall structure of a knowledge domain by highlighting the connections between research themes. Keywords from both Web of Science and Scopus are utilized to generate keyword co-occurrence networks. Figure 4 appears to be a visualization of the co-occurrence network and keyword relationship in a scientific field. The nodes represent various concepts or topics, and the connection between them indicates the strength of their

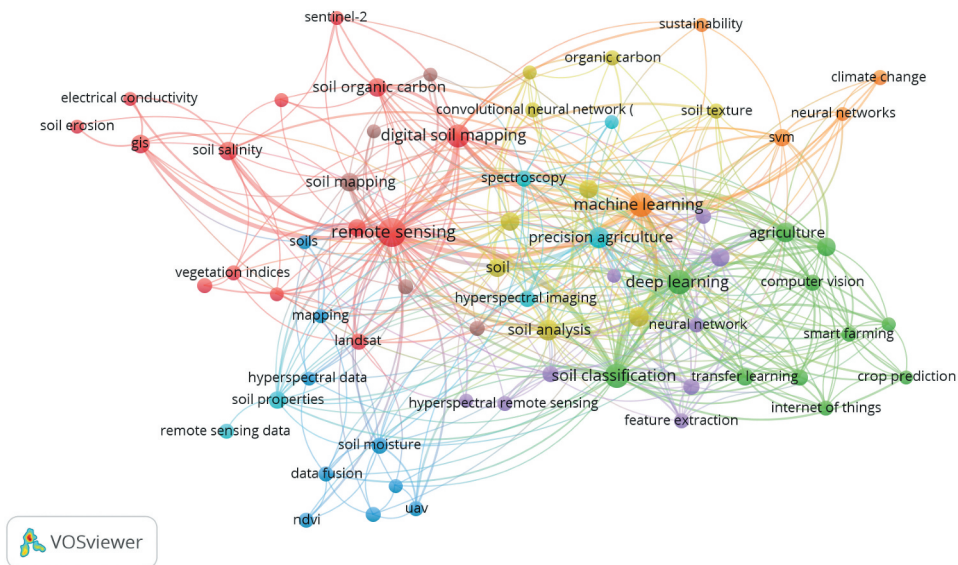


Figure 4. Keyword co-occurrence network visualization.

co-citation or co-occurrence in the literature. The central node, 'Soil', seems to be the core focus, with numerous related topics branching out from it. These include soil properties, soil analysis, soil mapping, soil classification, soil organic carbon (SOC), and soil texture, among others. The connections between these nodes suggest that they are closely linked in the scientific research and literature. This graph also highlights the interdisciplinary nature of this field, with connections to remote sensing, machine learning, agriculture, computer vision, neural networks, and climate change, indicating the diverse range of techniques and applications involved. Also emerging technologies like the presence of keywords like 'machine learning', 'deep learning', 'convolutional neural network', and 'internet of things' suggest that emerging technologies are being increasingly applied in this domain. The connection between the nodes indicates the strength of their co-citation or co-occurrence in the literature, providing insights into the relationships between different concepts and research areas. Further, the size and positioning of the nodes suggest the relative importance and centrality of each concept within the network, which can be useful for identifying key research areas and trends. The word cloud image extracted by R Studio with the biblioshine library depicted by [Figure 5](#) represents the most frequently occurring terms related to remote sensing, soil analysis, and environmental monitoring, where the size of each word indicates its frequency or importance. The dominant themes include remote sensing and soil analysis, highlighting the significant role of satellite imagery and aerial data in examining soil properties, land use, and environmental changes. Key concepts such as soil classification, soil moisture, soil property, soil pollution, and organic carbon suggest a focus on understanding soil characteristics, fertility, and contamination. The presence of terms like ML and DL indicates the growing use of artificial intelligence in soil studies, aiding in soil classification, prediction of soil properties, and detection of degradation. Additionally, the word cloud emphasizes environmental monitoring, agriculture, climate change, and ecosystems, signifying the broader impact of soil research on sustainability and climate studies. Geographic insight, such as the

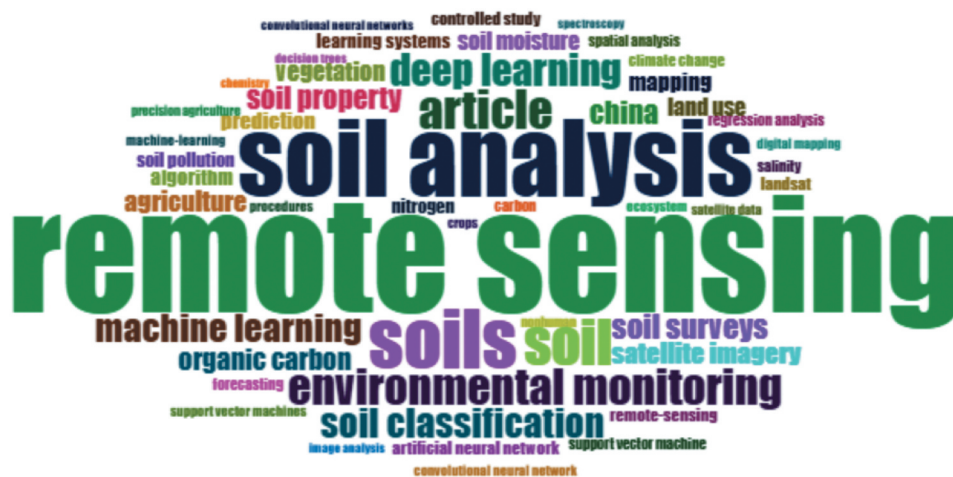


Figure 5. Occurrence and significance of keywords.

mention of China, suggests active research in this region, while methodologies like satellite imagery, Landsat, spectroscopy, and digital mapping highlight the tools used for soil assessment. Overall, the word cloud reflects the intersection of remote sensing, AI-driven analysis, and soil research, showcasing how advanced computational techniques are transforming soil health monitoring, precision agriculture, and environmental conservation.

As shown in Figure 6, this type of network visualization is widely been used in academic research to analyse author collaborations and citation relationships within a specific research domain. As in this network, each node represents an author in the research field. The size of a node is proportional to the number of times the author has been cited in the dataset. Larger nodes indicate highly cited authors as Minasny B., Dematte and Zhang Y. The connections between nodes indicate co-citation relationships, meaning that two authors have been cited together in multiple research papers. Thicker lines represent stronger co-citation relationships. Different colours represent distinct research groups or communities, as shown in co-citation, three colours blue, green, and red, which are formed based on how frequently authors are co-cited together. Now the significance of the co-citation network is that it helps to identify influential authors as the, largest node represents the most influential researchers in the field, helping scholars to recognize key contributors and colour-based clustering shows group of researchers who work on similar topics. Strongly connected authors often work in related areas, and identifying these relationships can help in finding potential collaborators. Researchers can use this visualization to discover major contributors and their citation relationships, streamlining the literature review process. Co-citation network visualization of authors is particularly useful in computer vision, remote

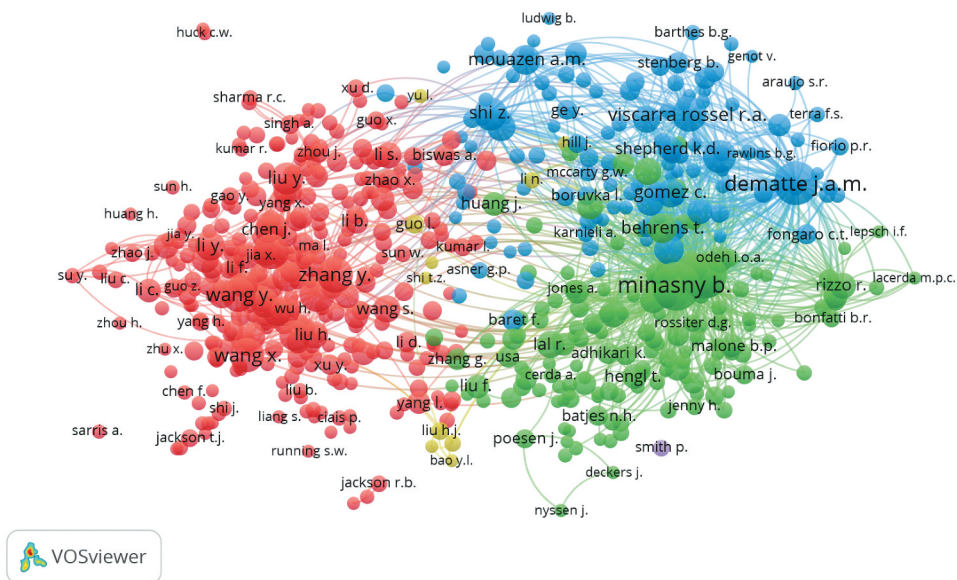


Figure 6. Co-citation network visualization of authors.

sensing, deep learning, and soil science research, as it helps scholars to understand the academic landscape and research impact.

5. Brief introduction of soil image datasets

In the domain of soil classification research, various databases have been utilized to facilitate comprehensive and comparative analysis. These soil image databases have been curated under diverse environmental conditions and lighting scenarios, tailored to the specific goals of each study. Researchers have utilized a variety of devices for image capture, ranging from digital single-lens reflex camera (DSLR) cameras to mobile phones. Significant differences in the configurations of image acquisition systems and the distances from which images are taken have been noted. Soil classification studies utilizing these images have been conducted in various regions, with datasets gathered from different countries and environments. This section presents an overview of several studies that have developed soil image databases under a range of conditions, accompanied by a comparative analysis of these databases in a tabular format as shown in [Table 1](#). Moreover, large datasets play a crucial role in mitigating the risk of overfitting, which happens when a framework learns the training data too well, leading to subpar performance on new and unseen data (Krizhevsky, Sutskever, and Hinton 2012; Lecun et al. 1998; Tran, Khoshelham, and Kealy 2019). With smaller datasets, models may become too focused on specific nuances, leading to these issues. In contrast, larger datasets provide greater variance, allowing models to train more comprehensively without succumbing to overfitting issue (Aydın et al. 2023; Gyasi and Purushotham 2023). A precise soil identification technique using deep learning requires a substantial set of ground truth datasets that have been manually labelled by experts, especially for multispectral images. This is crucial for maintaining the accuracy and dependability of the identification techniques.

Han et al. (2016) developed a soil image database using well-defined methodological approach to support soil analysis and classification. The researchers employed a Nikon D7000 SLR (Nikon corporation, Japan) camera to capture the soil samples, equipped with a Complementary Metal Oxide Semiconductor) sensor featuring effective pixels and a focal length range of 18 mm and 105 mm, as shown brightness was adjustable in [Figure 7](#). This study proposed a smartphone-based soil colour sensor for rapid soil type classification. Ten standard soil types (latosol, red, yellow, burozem, drab, podzolic, chernozem, desert, paddy, and purple soils) were obtained from the Department of Geography, East China Normal University, China. To validate the approach, 500 additional soil samples were collected from different regions of China and measurements were performed using an AvaSpec-2048 spectrometer (Avantes Company, Dutch) (200 nm–1100 nm range, Czerny – Turner optics) and AvaLight-DH-S-DUV (Avantes Company, Dutch) is a light source the wavelength range of the light source was 190–2500 nm. Each soil type was scanned 200 times and average spectral revealed the distinct reflectance characteristics. Further, RGB values were extracted and averaged using MATLAB 7.0. A Xiaomi 2s smartphone (13 MP Sony Exmor RS CMOS) was adapted with external lenses, a shading device, and a green calibration card in the experimentation. The flash served as a light source, and a custom Android

Table 1. Digital soil image datasets.

Author	Data composition	Location	Capturing Device
Han et al. (2016)	Soil image database with ten images per specimen under controlled LED illumination.	Beijing, China	Nikon D700 DSLR, Xiaomi 2S
Honawad et al. (2017)	Soil sample images were captured using a camera mounted over a light vestibule.	Not specified	Sony DXC-3000A camera)
Sudarsan et al. (2018)	A total of 123 soil sample were gathered from two fields, with three images taken per sample and three on-site images captured from 67 locations.	Quebec, Canada	AD-7013MT USB Digital Microscope (5MP)
Dornik, Drăgut, and Urdea (2018)	Ten soil types classified using SPOT DEM and Landsat 8 imagery.	Western Romania	Various satellite data source
Barman et al. (2018)	50 soil images from ten paddy fields, five samples per field.	Guwahati, India	Xiaomi Redmi 3S Prime (13MP)
Maniyath et al. (2018)	Soil images database from Munsell color chart (256×258 pixels).	Not specified	13MP smartphone camera
Shukla et al. (2018)	35 digital layers of environmental covariates from satellite sources.	Not specified	Various satellite data sources)
de Oliveira Morais et al. (2019)	189 digital images of sieved, dried soil samples, three images per sample (2048×1536 pixels).	Not specified	Leica EZ4 stereo microscope
Inazumi et al. (2020)	1,000 soil images categorized by particle size (clay, sand, gravel), varying illumination.	Not specified	iPhone 7 (12MP), FUJIFILM X-T4
Barman and Choudhury (2020)	40 soil images captured under visible light, 10-inch distance.	Guwahati, India	Redmi 3S Prime (4160×2340)
Azizi et al. (2020)	Stereo images for soil classification, unaffected by ambient light variations.	University of Mohagegh Ardabili, Iran	W3-Fujifilm stereo camera (10MP CCD sensors)
Jiang et al. (2021)	160 soil profiles grouped into 5 classes (128×128 pixels).	Liaoning and Inner Mongolia, China	Canon EOS 50D/60D, Nikon D7000, Huawei Honor 6 Plus
Uddin and Hassan (2022)	76 images from eight soil types, total 608 images.	Mymensingh, Bangladesh	Samsung Galaxy A20 (13MP, 4160×3120)
Padmapriya and Sasilatha (2023)	5,938 soil images across four soil types.	Manalur, Vriddhachalam Taluk, Tamil Nadu	Smartphone
Gyasi and Purushotham (2023)	4,864 RGB soil images (224×224 pixels, PNG format) from nine categories under various weather conditions.	Various States, India	Smartphones and digital cameras
	Samples from Godavari River, including those from the coastal region (characterized alluvial and sandy soils) and drought-prone areas (dominated by rocky soils).	Godavari River coastal zone, Mandanapalle, India	48MP smartphone camera (ISOCELL GM2 sensor)

application handled image capture and RGB calibration. Noise was reduced by simultaneous capture of soil and calibration card with corrected RGB values, which were computed as:

$$RGB_{\text{calibrated}} = \left| \frac{RGB_{\text{soil}N_1} + \dots + RGB_{\text{soil}N_2}}{N_2 - N_1 + 1} - \frac{RGB_{\text{card}N_1} + \dots + RGB_{\text{card}N_2}}{N_2 - N_1 + 1} \right|$$

where $RGB_{\text{soil}N}$ and $RGB_{\text{card}N}$ are respectively the RGB values of the calibration card and the soil sorted by the Matlab7.0 software and $N_1 = 20,000$, $N_2 = 50,000$. The calibrated RGB values were classified using linear discriminant analysis (LDA). The smartphone-based sensor achieved more than 90% identification accuracy across soil types, with rates ranging from 94% (Chernozem) to 100% (Yellow and Burozem

Table 2. Evaluation of various image processing and computer vision techniques for soil categorization efficiency.

Reference	Method	Approach	Highlights and Shortcomings
Krishna Murti and Satyanarayana (1971)	Color development analysis	Multi regression correlation analysis of soil color and chemical characteristics	Highlights: Identified key factors (titanium and ferrous iron) influencing soil hue; partial regression analysis clarifies contributions of clay and organic matter to soil color. Shortcomings: Results may be specific to basaltic soils of the Malwa plateau; generalizability to other soil types may be limited.
Zhang, Younan, and King (2003)	Wavelet-based system	wavelet transform for feature extraction, ML classifier, FLDA	Highlights: Effective in capturing local and global textural information; enhance efficiency and accuracy; tested on sand, silt, and clay. Shortcomings: May require extensive sample data for training; performance can vary with soil type and texture complexity.
Aydemir, Keskin, and Drees (2004)	Automated mineral classification	Thin section method for automated classification of mineral and non-mineral constituents using a color image flatbed scanner	Highlights: Achieved greater than 95% accuracy in separating and quantifying five distinct classes; employs unsupervised nearest neighbor classification. Shortcomings: Specific limitations not detailed; may require further optimization for diverse soil types.
Zhang, Younan, and O'Hara (2005)	Hyperspectral classification	Hyperspectral soil signature, wavelet domain statistical models (ML, HMM)	Highlights: Rich information from hyperspectral data; robust classification; HMM classifier achieves high accuracies (100%,97%,89%,97%,100% for different textures). Shortcomings: The complexity of hyperspectral data processing; May still struggle with certain soil texture variations.
Sofou, Evangelopoulos, and Maragos (2005)	Modern computer vision integration	Image feature extraction, texture analysis, segmentation using morphological PDE-based methods	Highlights: Sophisticated approach for soil micromorphology; enables further interpretation of soil images through joint segmentation and feature measurement. Shortcomings: Complexity may require advanced computational resources; effectiveness may depend on specific soil characteristics.
Breul and Gourves (2006)	Comprehensive soil characterization	Global image analysis for texture analysis and soil characterization.	Highlights: Effectively characterized 80m fine grained materials; provides insights into relationship among particle size distribution, mineralogy, water content, and compaction. Shortcomings: May require extensive data for comprehensive analysis; effectiveness may vary with soil complexity.

(Continued)

Table 2. (Continued).

Reference	Method	Approach	Highlights and Shortcomings
Botelho et al. (2006)	Soil color determination	Comparison of soil color using Munsell charts and colorimetry	Highlights: Strong correlation between Munsell Chart and colorimeter measurement; colorimeter mitigates psychophysical errors in visual assessments. Shortcomings: Visual comparison may still introduce subjectivity; and reliance on specific soil characteristics from the study area.
Bogrekci and Godwin (2007)	Non-contact clod size assessment	Computer vision technique for measuring clod and overall size distribution in the field	Highlights: Achieved a dimension assessment root-mean-square error of 14mm; utilized digital image processing methods to address geometric and quality distortions. Shortcomings: Limited to sandy loam soils; may require further validation across different soil types and conditions.
O'Donnell et al. (2010)	SRF identification and quantification	Digital camera and image classification software for identifying and quantifying SRF	Highlights: Achieved 99.8% accuracy in color determination; minimal changes in identified SRFs after multiple rewetting applications; increased area of Low Chroma observed in several horizons. Shortcomings: Limited to specific landscapes in Missouri; results may vary with different soil moisture conditions.
Shenbagavalli and Ramar (2011)	Preprocessing and feature extraction	Gray-level thresholding, low-pass filtering, edge enhancement, 3×3 Law's mask convolution	Highlights: Efficient and effective for automated soil classification; demonstrated on diverse soil textures. Shortcomings: May require careful tuning of preprocessing steps; effectiveness can depend on the quality of initial images.
Chung et al. (2012)	RGB histogram analysis	In-situ classification system and image processing using RGB histogram	Highlights: High accuracy in classifying soil textures with a squared correlation coefficient of 0.96; image processing produced consistent results with laboratory methods for 48% of samples. Shortcomings: Limited to Korean paddy soil series; may require further validation across different soil types.
Han et al. (2016)	Smartphone based soil color classification	Low-cost smartphone based miniaturized sensor for soil color classification using machine vision and visible spectrum	Highlights: Achieved 100% identification accuracy for yellow soil and burozem soil; straightforward and affordable design. Shortcomings: Challenges in managing ambient light and machine parameters.

(Continued)

Table 2. (Continued).

Reference	Method	Approach	Highlights and Shortcomings
Ajdadi et al. (2016)	Real-time tillage quality assessment	Algorithm for assessing tillage quality using image processing with various camera heights	Highlights: Achieved 72.04% accuracy for ANN classifier at 60cm height; effective in estimating mean weight diameter of soil aggregates with over 80% accuracy. Shortcomings: May require extensive data handling; accuracy may vary with different soil aggregate sizes.
Honawad et al. (2017)	Signal processing methods	Low mask, Gabor Filter, color quantization for image enhancement and texture feature extraction.	Highlights: Effective retrieval performance; superior classification rates based on a dataset of 100 soil images from 10 distinct types. Shortcomings: Limited to the specific types of soil images used; may require additional methods for broader applicability.
Gurubasava and Mahantesh (2018)	pH value determination in agricultural soil	Digital image processing techniques to identify and analyze the pH value of agricultural soil using RGB index values and PCA	Highlights: Achieved 100% accuracy for trained images and 91% for untrained images; reflects attributes such as mineral content and organic matter. Shortcomings: MSCC can be challenging to apply effectively; may require further validation across different soil types.
Maniyath et al. (2018)	Soil color detection	Efficient algorithm for detecting soil color through digital image processing	Highlights: Accurately determines soil color by isolating the soil portion from the background in selected images. Shortcomings: Specific limitations not detailed; further validation may be needed for diverse.
Pethkar (2018)	Feature extraction techniques	Color moments, HSV wavelet transforms, Gabor filters for texture feature extraction; classification using SVM and ANN	Highlights: Achieved 100% accuracy in classifying soil types; flexible methodology allowing substitution of SVM with ANN for classification tasks. Shortcomings: May require extensive computational resources; effectiveness may depend on the quality of input images.
Sudarsan et al. (2018)	CWT-based computer Vision algorithm	CWT for particle size analysis from digital images.	Highlights: Strong correlations with laboratory measurements; achieved 87% and 88% prediction accuracy for coarse and fine fractions; shows promise as a proximal soil sensor. Shortcomings: Weaker predictions from in-situ images (48% for coarse, 56% for fine) due to field conditions; further research needed.
De Oliveira Morais et al. (2019)	Digital image processing and MIA	Predicting and classifying soil texture using digital images and multivariate regression	Highlights: Achieved 100% match with standard classification; cost-effective, environmentally friendly, and significantly faster than traditional methods. Shortcomings: Relies on accurate image processing; effectiveness may vary with sample preparation and image quality.

Table 3. Deep learning and machine learning techniques for soil classification and mapping.

Reference	Method	Approach	Highlights and Shortcomings
Reale et al. (2018)	Atuomaed Fine-Grained Soil classification	Feed forward ANN with CPT measurements	Highlights: Achieved nearly 90% accuracy; reduced time and costs; outperformed standard models; confirms relationships between CPT and results and soil properties. Shortcomings: Limited generalizability to other soil types; dependency on quality of CPT data.
de Oliveira Morais et al. (2019)	MIA approach for SOC measurement	least square SVM with digital image analysis	Highlights: Strong correlation ($R^2 > 0.93$) between image data and SOC; eco-friendly cost-effective, and rapid alternative for soil testing. Shortcomings: May require extensive image preprocessing; performance may vary with different soil types.
Singh and Kasana (2019)	Soil property quantification	LSTM network with PCA	Highlights: Highest R^2 of 0.94 for organic carbon; effective comparison with PLSR, SVR, PCR, MLR, and SWR; vital for sustainable land management. Shortcomings: Potential overfitting with limited data; reliance on high-quality hyperspectral data.
Yu et al. (2019)	3D-CNN for soil classification	3D-CNN with liquid crystal tunable filter.	Highlights: Utilizes compressive sensing for Hyperspectral image reconstruction; employs PCA for dimensionality reduction; introduces a differential perception model for feature extraction. Shortcomings: Dependence on low spatial resolution detectors; potential challenges in real-time processing; complexity of the model may hinder practical applications.
Y. Liu et al. (2024)	LSTM-CNN-Attention Model	LSTM-CNN Attention model utilizing LUCAS soil dataset.	Highlights: Impressive R^2 values: 0.949 (OC), 0.916 (N), 0.943 (CaCO_3), 0.926 (pH); RPD values exceeding traditional and deep learning models; enhances accuracy and reliability of soil property predictions. Shortcomings: Complex model architecture may require significant computational resources; performance may be sensitive to hyperparameter tuning.
Gupta et al. (2024)	Advanced Deep Learning model for soil classification	Deep-learning model integrated within a space station and rover system	Highlights: Achieves approximately 80% test accuracy; reliable and precise soil categorization in space informatics; facilitates efficient decision making. Shortcomings: Accuracy may be insufficient for critical applications; reliance on data transmission may introduce latency; potential limitations in diverse soil conditions.
El-Rawy et al. (2024)	Salinity Detection and Segmentation	MU-NET with remote sensing data	Highlights: Achieved accuracies of 91.27% for salinity and 90.83% for vegetation; utilizes 91 and Landsat 8 images over ten years; superior performance compared to existing methods; highlights spatial distribution of salinity and vegetation decline. Shortcomings: Relies on satellite image quality; potential limitations in model generalization to different geographical areas; may require extensive computational resources for processing.

(Continued)

Table 3. (Continued).

Reference	Method	Approach	Highlights and Shortcomings
Ke, Ren, and Yin (2024)	Soil property prediction with TRNN	Six-layer CNN with encoder-decoder architecture	Highlights: Achieved R^2 values exceeding 0.93 for cation exchange capacity, organic carbon, calcium carbonate, pH clay, silt, and sand content; surpassed traditional and deep learning methods; utilized various interpretative techniques for model outputs. Shortcomings: Mutitask structures reduced efficacy; reliance on high quality spectral data; may require significant computational resources for training and validation.
Saberioon et al. (2024)	Soil organic Prediction	1DCNN and FCNN with SAE	Highlights: SAE-DL model outperformed traditional methods, achieving R^2 of 0.78 and RMSE of 3.94%; demonstrated superiority of 1DCNN over FCNN; Utilized data from LUCAS database. Shortcomings: Performance may be limited by the quality of spectral data; reliance on feature extraction may introduce biases.
H. Guo et al. (2025)	Multimodal fusion for soil classification	Multimodal deep learning models with various fusion strategies	Highlights: Generated 23,122 labelled entries from diverse data types; intermediate fusion strategies outperformed late fusion; highest accuracy exceeding 0.99 on the test set; uncovers correlations among diverse soil data. Shortcomings: Complexity of multimodal data integration; potential challenges in data augmentation; may require extensive computational resources for training
Y. Zhao and Teng (2025)	Soil layer classification with AB-SMOTE	AB-SMOTE and PSO-RF	Highlights: Effectively addresses dataset imbalances; produces high-quality synthetic samples; substantial improvements in classification accuracy, precision, and recall. Shortcomings: Dependence on the quality of initial data; potential computational overhead from the PSO-RF model; may require careful tuning of parameters for optimal performance.

soils). The performance was consistent with DSLR and spectrometer-based methods, demonstrating the feasibility of low-cost and portable soil classification (Han et al. 2016).

Honawad *et al.* (2017) introduced a digital image processing approach for soil classification and suitable crop prediction. A dataset of 100 soil images, representing 10 different soil types (red, clay, river, sea, alluvial, black, silt, and their mixtures) was acquired using a Sony DXC-3000A camera under controlled fluorescent illumination. The captured images underwent shade correction and artefact removal to improve the visual quality.

- (1) Colour features: RGB components and quantization levels were computed.
- (2) Boundary descriptors: Colour quantization, gabor filter, and the law mask S5S5 are used to extract the features of the query image and the training images. Next, the database's training photos are compared to the soil's query image. The result is the

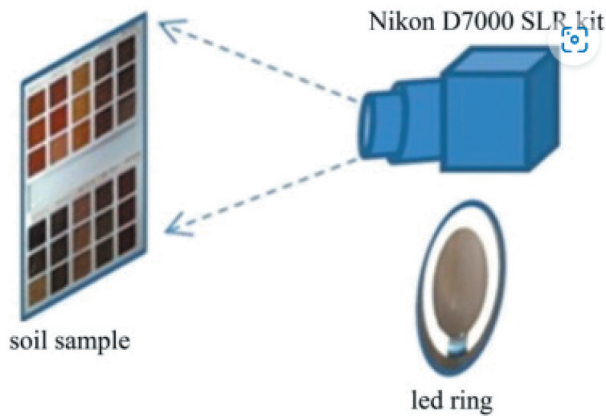


Figure 7. Soil image dataset extraction using a device (Han et al. 2016).

soil with the highest matching ratio based on the query and training image matching.

The proposed approach applies effective feature extraction techniques, such as texture-based feature extraction, which is accomplished by applying a law mask (S5S5), Gabor filter, and colour quantization for colour-based feature extraction. The matching is then accomplished by using statistical metrics such as the mean, standard deviation, kurtosis and skew. It has been demonstrated that the suggested approach, which employs a Gabor filter, performs better. The accuracy of the algorithm is improved by combining several colour and texture features that are taken from the photos. The system effectively recognized soil types and demonstrated potential for guiding suitable crop prediction (Honawad et al. 2017).

Dornik Drăgut, and Urdea (2018) study area for soil type mapping was located in the western part of Romania, covering 318 km² in the administrative territory of Vermes, Darova, and Ramna communes. The region includes the piedmont hills, elevated plains, and the poganis floodplain with elevations varying between 100 to 510 meters and slope inclinations generally below 10. The underlying Geology primarily consists of sedimentary and metamorphic rock formations. The meteorological traits are classified by an average yearly temperature of 10.5C and an average yearly precipitation of 631 mm, with increased rainfall influenced by the closeness to forested areas. The authors utilized a Satellite Pour l'Observation de la Terre digital elevation model, a Landsat 8 satellite image, and a topographical database incorporating 171 soil outlines with Geospatial points and soil classification aligned with the Romanian soil taxonomy system (RSTS). Ten soil types were identified in accordance with the RSTS (2012) and the world reference base for soil resources (IUSS Working Group WRB, 2014). The soil categorization level was streamlined to ensure a manageable number of soil outlines for each category, since initially soil classifications were extensive with several categories having only one or two corresponding soil outlines (Dornik, Drăgut, and Urdea 2018).

Sudarsan *et al.* (2018) developed a computer vision approach using continuous wavelet transform (CWT) for soil texture characterization from microscope-captured digital images. A low-cost portable microscope (5MP, 200× magnification) was employed to acquire images of air-dried, ground soil samples (123 images) collected from two agricultural fields with variable soils. Additional in-situ images were obtained at 67 locations after residue removal. The images were converted to greyscale, and CWT was applied along rows and columns to capture scale-specific variations. The total area under the global wavelet spectrum was used to estimate particle size fractions: coarse (2.0–0.05 mm) and fine (< 0.05 mm). These estimates were compared with hydrometer-based measurements, showing strong agreement. For laboratory samples, prediction accuracies were high (87–88%) with RMSE values between kg^{-1} for both coarse and fine fractions. The method demonstrated potential as a low-cost, portable soil texture sensing tool. However, in-situ images yielded weaker predictions (48–56%), primarily due to image quality issues under field conditions, highlighting the need for further refinement. Only the CWT has been used in this investigation. In contrast to CWT, the discrete wavelet transform (DWT) analyzes scales in octaves, which are integer powers of two, rather than voices, which are fractional powers of two. A physically relevant study of scale may not always be possible with octave sampling. The size of the object being observed – in this case, coarse particle sizes – has a direct correlation with wavelet scale information. Thus, CWT was selected instead of DWT. Briefly, for a spatial series Y_i of length N (where $i = 1, 2, 3, \dots, n$), the CWT coefficient $W_i^Y(s)$ can be calculated as follows:

$$W_i^Y(s) = \sqrt{\frac{dx}{s}} \sum_{j=1}^N Y_j \psi\left(\frac{(j-i)dx}{s}\right)$$

where, dx represents the equal sampling interval of the translated wavelet x , s is the scaled wavelet, and ψ is the wavelet function (Sudarsan *et al.* 2018).

Barman *et al.* (2018) investigated the prediction of soil pH using HSI colour image processing combined with regression analysis. A total of 40 soil samples were taken from the top 6 inches of soil which were collected from different regions of Guwahati, Assam, India. The soil images were captured using a Redmi 3s Prime smartphone camera (4160 × 2340 resolution) under controlled visible light conditions to ensure the consistency. The laboratory pH measurement was performed using a calibrated pH meter (pH 7 buffer solution standard), and each test was conducted by mixing 20 g of soil with 40 ml of distilled water with stirring solution. The image preprocessing steps included contrast enhancement, resizing, and filtering. Regions of interest (ROI) were extracted using binary masking. Feature extraction involved conversion from RGB to HSV color space, where the saturation HSV was selected as the primary predictor of soil pH:

$$\text{ColorIndex} = \text{SaturationHSV}$$

Regression modelling: A linear regression was fit to relate the colour index to laboratory measured pH values:

$$y = 46.01113x + 4.95556$$

This is coefficient of regression analysis of the Guwahati so that a good mixture soils are comes out. We discovered a correlation accuracy of 84.9% after using linear regression

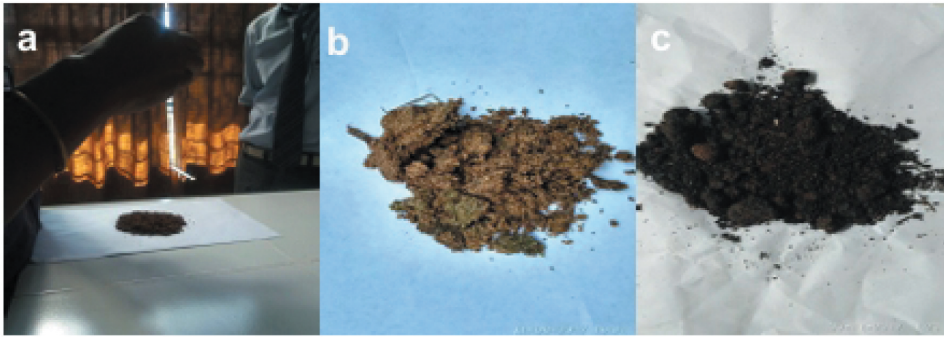


Figure 8. (a) Soil images captured by Redmi 3S Prime smart phone. (b) Soil sample image (c) soil sample image (Barman et al. 2018).

between soil pH and saturation value, indicating a linear relationship between the two. Nevertheless, the correlation coefficient rose to 86% when quadratic regression was applied. This indicates that in the Guwahati area of Assam, quadratic regression offers a little superior forecast for soil pH. As shown in Figure 8, the image acquisition procedure involved photographing five soil samples from each and every field, resulting in a total number of 50 soil samples being collected and used (Barman et al. 2018).

Maniyath et al. (2018) created a soil image database using the Munsell soil colour chart (MSCC) as source. The study developed a soil colour detection framework using digital image processing and K-nearest neighbour (KNN) classifier. Images of the MSCC were captured using a 13 MP digital camera. Each colour patch was cropped to the size of 256×256 pixels. The RGB values of each patch were extracted and summarized using the mode of R, G, and B channels to construct the training dataset.

- (1) Image Acquisition: Soil samples were photographed under consistent illumination.
- (2) Filtering: The median filter is employed for filtering. It is a spatial, nonlinear filter and uses a square window for filtering. The equation of median filter:

$$Y_{ij} = \text{median}\{X_{i+s, j+r} | (s, t) \in \omega\}$$

Y_{ij} denotes the output of the median filter for a given pixel X_{ij} . Here, (s, t) indicates the pixel position within the scanning window.

- (3) Segmentation: Images were converted from RGB to HSV colour space, and thresholding on the hue (H) channel isolated the soil region. The RGB to HSV conversion formulas are given below:

$$H = \cos^{-1} \left\{ \frac{\frac{1}{2} [(R - G) + (R - B)]}{\sqrt{(R - G)^2 + (R - B)(G - B)}} \right\}$$

$$S = 1 - \frac{3}{R + G + B} [\min RGB]$$

$$V = \frac{1}{3}(R + G + B)$$

- (4) Classification: soil samples were classified using the KNN algorithm, where the Euclidean distance was applied.

The ability to sense colour is crucial for determining the properties of the soil in a particular location. This project's goal is to use MATLAB for digital image processing in order to identify the colour of the soil. A KNN classifier assigns relevant Munsell soil notations to the photos based on their RGB values once the soil is separated from the background using HSV segmentation (Maniyath et al. 2018).

Shukla et al. (2018) implemented the random forest (RF) classifier for soil spatial prediction and compared its performance against two baselines: classification and regression tree (CART); CART with decision tree (CDT) and CART ensemble bagger (CEB). Soil-forming factors (scorpan model) were used as a predictors to classify 11 soil categories in Indian districts. A total of 35 digital layers were prepared, combining: (i) satellite data (Advanced Land Observing Satellite (ALOS) digital elevation model, Landsat-8, Moderate Resolution Imaging Spectroradiometer (MODIS) normalized difference vegetation index (NDVI), Radar Imaging Satellite-1 (RISAT-1), Sentinel-1A), and (ii) climatic covariates (annual precipitation and temperature). RF hyperparameters were tuned by maximizing Cohen's kappa (κ), while minimizing the number of random split variables. Noise stability was tested by introducing false labels in 5% increments and by progressively reducing the training dataset size. Models were implemented in MATLAB (RF-matlab package). The large datasets were partitioned and mosaicked, and a 4×4 majority filter was applied to reduce pixel noise. In last, the model performance was evaluated using accuracy-related indices. RF consistently achieved the highest accuracy and κ values compared to CDT and CEB, respectively. Accuracy declined only when more than 60% of training data was removed, while CDT and CEB degraded at 45% and 25%, respectively. RF also demonstrated stronger resistance to noisy labels, making it more reliable for large-scale soil category mapping (Shukla et al. 2018).

De Oliveira Morais (2019) employed a specific methodology for generating and capturing soil sample images. Five municipalities in three Brazilian states provided a total of 63 topsoil samples (0–10 cm depth, 500 g each), the majority of which came from Nova Canaã do Norte (Mato Grosso). Samples were prepared for granulometric examination by being dried for 48 hours at 45°C, crushed, and sieved (less than 2 mm). The standard pipette method was used to determine the particle size distribution after chemical and physical dispersion, and the difference was used to compute silt. The soils were primarily categorized as clay and had median values of 40 g/kg sand, 58 g/kg clay, and 2 g/kg silt, which are characteristic of humid tropical climates. A Leica EZ4D stereo microscope with an integrated digital camera was used to picture 2 g of sieved soil in triplicate for image analysis, yielding 189 TIFF RGB images 2048×1536 . RGB, grayscale, and HSV colour spaces were used to represent the images. A thorough description of the colour characteristics of soil was made possible by the conversion of RGB photos (16.7 million colours) to grayscale and HSV, which together produced around 1,792 variables per image (de Oliveira Morais et al. 2019).

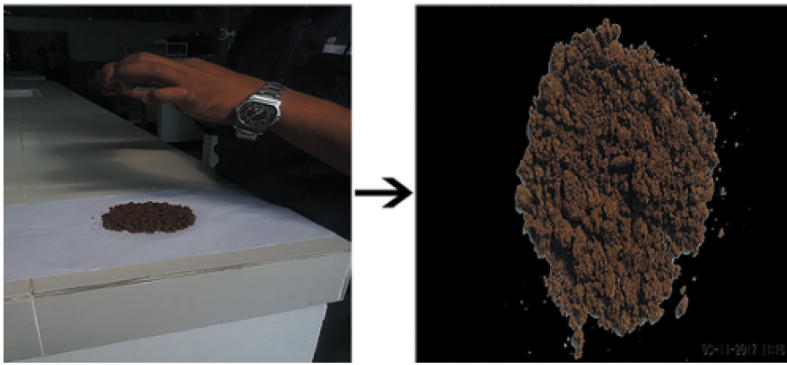


Figure 9. Soil sample collection and its ROI after segmentation (Barman and Choudhury 2020).

Barman and Choudhury (2020) employed a specific methodology for capturing the soil sample image. The researchers used a Redmi 3s prime smartphone camera to capture the soil images, which had a resolution of 4160×2340 pixels. The soil samples were photographed under visible light conditions and the gap between the soil surface and the camera was maintained at 10 inches to avoid uncontrolled illumination as shown in Figure 9. The study developed a low-cost, image-based framework for soil texture classification using multi-class SVM. A total of 50 soil samples were collected from 10 paddy fields in West Guwahati, Assam, India, at 200 m intervals and 6 inches depth. The soil texture was determined using the hydrometer method and the USDA soil texture triangle, yielding 12 classes (e.g. clay, clay loam, sandy clay loam, silt loam, etc.). Images collected were contrast-enhanced, denoised using a low-pass Butterworth filter with a cut-off frequency 0–0.5 and resized to 300×400 pixels. ROI were segmented using Gabor filters (4 scales and 6 orientations). Multiple descriptors were extracted: HSV histograms (32 bins), color autocorrelogram (64 features, color moments (3 for mean, 3 for standard deviation, and 3 for skewness; total 9 features), Gabor features (24 for mean squared energy and 24 for amplitude; total 48 features), discrete wavelet transform (DWT) features (20 for mean and 20 for standard coefficients; total 40 features). The final feature vector contained 193 features per image. A multi-class SVM with a linear kernel was implemented in MATLAB (R2015a). Data were split into 29 training samples and 24 testing samples across 12 soil classes. For three-class classification (clay loam, sandy clay loam, and silt loam), the model achieved an average accuracy of 95.72%. For twelve-class classification, the average accuracy was 91.37%, with the highest accuracy for loam (96.84%) and clay loam (96.20%), and slightly lower for loamy sand (81.25%) and silty clay (84.25%). The system demonstrated higher efficiency compared to conventional hydrometer-based classification and offered a rapid, smartphone-based solution for soil assessment (Barman and Choudhury 2020).

Inazumi et al. (2020) used a dataset of 1000 soil images to classify soil types. The soil samples were classified according to their particle size, which was adjusted through sieving, into three categories: clay ($D_{50} = 0.008$ mm), sand ($D_{50} = 0.7$ mm), and gravel ($D_{50} = 4$ mm). Unlike the previous studies, the soil samples were arranged in a transparent reusable plastic tumbler. The images were obtained using an iPhone 7 smartphone, equipped with a 12-megapixel camera, whereas, a FUJIFILM X-T4 digital camera with a 26-

megapixel sensor was available at the time. The image sensor size of the iPhone 7 is 4.8×3.6 mm, while the FUJIFILM X-T4's sensor measures 23.5×15.6 mm, which affects image noise and accuracy. The photographs were captured indoors, with 200 photographs captured for the clay samples (with and without illumination), 200 photographs for the sand samples (with and without illumination), and 100 photographs for the gravel samples (with and without illumination), resulting in a total of 1,000 soil images. A CNN was implemented in Python (3.6.6) with TensorFlow (1.9.0). The architecture included two convolutional layers, two pooling layers, and one fully connected layer. The images were resized to 56×56 pixels and converted to grayscale. Training was performed with a good learning rate, batch size = 20 and 70 epochs. The steepest descent method with back-propagation used to minimize the error function as:

$$E = \frac{1}{2} \sum_{i=1}^n (o_i - t_i)^2,$$

where, o_i is the model output and t_i is the teacher signal (Inazumi et al. 2020).

The dataset was created by Azizi et al. (2020) for real-world applications rather than controlled laboratory settings, utilizing stereo images for this purpose. Stereo imaging offers two key advantages: it remains unaffected by ambient light variations and allows image capture in various field conditions including both sunny and cloudy days. This flexibility enhances the image acquisition process. Despite potential overlaps in stereo pairs, the limited spatial differences between the images enable the developed model to be designed to efficiently derive attributes. In this research, a W3-Fujifilm stereo camera, equipped with dual 10-megapixel charge couple device sensors for the left and right lenses, was employed. The camera had a baseline spacing of 7.5 cm and a focal length of 12 mm, with the lens positioned 60 cm above the ground. This height was chosen to facilitate the classification (Azizi et al. 2020).

Firman Ghazali et al. (2020) integrated remote sensing (Landsat 8 OLI/TIRS imagery), field sampling, and laboratory analysis to estimate soil moisture, salinity, and pH in paddy fields of the Citarum River Basin, Indonesia. Soil samples ($n \approx 100$) were collected from bare soil and paddy-planted areas, and laboratory analysis determined soil pH, moisture, and salinity. Satellite images and field surveys were used to estimate soil pH and its relation to soil moisture and salinity. Three multi-temporal Landsat 8 images (path 122, row 65) were downloaded from the U.S. Geological Survey Earth Explorer and analyzed. A field survey collected 100 soil samples, where pH was measured directly in situ using a 4-in-1 portable digital device at 20 cm depth. For harder soils, samples (250 g) were taken to the laboratory and analyzed for pH, moisture, and salinity using Kalium Chloride extraction. Additional GIS data, including land cover maps and sampling points were digitized from Google Earth to separate paddy fields from other land uses. The study focused only on pH, moisture and salinity, while other soil properties were not considered. Soil moisture was estimated using the soil moisture index (SMI), derived from NDVI and land surface temperature:

$$SMI = \frac{(TS \text{ Max} - LST)}{(TS \text{ Max} - Ts \text{ Min})}$$

$$TS_{Max} = a1 * NDVI + b1$$

$$TS_{Min} = a2 * NDVI + b2$$

Soil salinity was calculated using the soil salinity index from Landsat short wave infrared bands. Soil pH was modelled using multiple regression, producing separate models for paddy leaf and bare soil conditions:

$$pH = 6.493 - 35.152B2 - 52.380B3 + 1.099B4 + 30.040B6 - 8.181B7,$$

$$pH = 6.232 - 59.439B2 - 89.326B3 + 136.721B4 + 5.612B6 - 25.603B7,$$

where, B2, B3, B4, B6, B7 are Landsat 8 spectral bands. Ground measurements were compared with model predictions. The performance was evaluated using RMSE and percentage RMSE (PRMSE):

$$RMS\ E = \sqrt{\frac{1}{n} \sum_{i=1}^n (X_1 - X_2)^2}, \quad PRMS\ E = \frac{RMS\ E}{\bar{X}_2} \times 100\%.$$

Soil moisture increased from $\sim 4\%$ to 8% over 30 days, while soil salinity rose from ~ -2 to 0.5 dS/m per 30 m^2 . Soil pH ranged between 2.12 and 7.59, with paddy leaf models producing higher values compared to bare soil models. The prediction accuracy was $RMSE = 1.40$ and $PRMSE \approx 24\%$, respectively. Regression analysis showed a weak negative correlation between soil pH and soil moisture ($R^2 = 8.37\%$ in bare soil; $R^2 = 100\%$ in paddy areas), and a moderate negative correlation between soil pH and salinity ($R^2 = 34.89\%$ in bare soils) (Firman Ghazali et al. 2020).

Uddin and Hassan (2022) profess that in research, soil samples were primarily collected from various locations in the Mymensingh division of Bangladesh, with additional samples sourced from an online soil dataset. The samples were gathered using a trowel from a depth of 0–15 cm and subsequently dried in the laboratory at 105°C . After drying, the samples were ground and placed on a paper surface for imaging. A Samsung Galaxy A20 smartphone equipped with a 13 MP camera was installed on a tripod at a 5 cm distance to acquire the visuals. A total of 76 images were taken for each soil type by regulating the paper layouts at various slants. The datasets consist of eight different classes: (i) agronomy, (ii) clay, (iii) compost, (vi) EPI, (v) loamy, (vi) SI, (vii) sandy and (viii) silt, organized alphabetically, leading to an initial total of 608 depictions ($76\text{ images} \times 8$ classes). Image augmentation techniques were then applied, resizing images across four scaling levels (4160×3120 , 2080×1560 , 1040×780 , and 520×390), rotating them at four angles (0, 90, 180, and 270), and reflecting them in both directions; i.e. horizontally and vertically. This augmentation process increased the number of images per soil class to 4,864 images ($76\text{ images} \times 64$ variations), leading to a comprehensive dataset of 38,912 soil images ($4,864\text{ images} \times 8$ classes) (Uddin and Hassan 2022).

According to the information provided by Padampriya and Sasilatha (2023), two recent studies have utilized smartphone-captured soil images for soil classification. In dataset, total of 5,938 soil images were captured, covering four soil types: clay, clayey peat, sandy clay, and humus clay. The soil samples were obtained from diverse ecological settings in Manalur, Vriddhachalam Taluk, Tamil Nadu, India. The

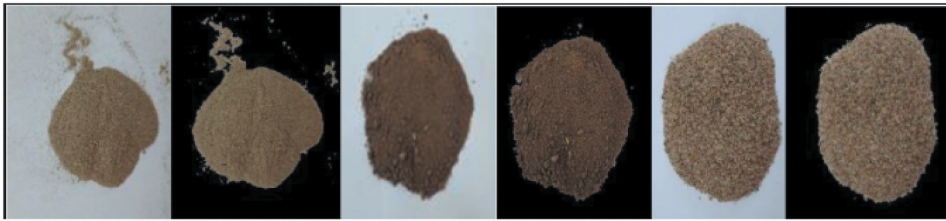


Figure 10. Ground truth VIT soil dataset samples: from top left to right; red soil, laterite soil, arid/desert soil, alluvial soil, saline soil, yellow soil, black soil, and forest soil (Gyasi and Purushotham 2023).

researchers employed a multi-tier integrated model, which integrated conventional machine learning and deep learning approaches, to categorize four distinct soil types (Padmapriya and Sasilatha 2023).

Gyasi and Purushotham (2023) conducted a review of 12 prominent research papers chosen from an initial selection of 150, concentrating on deep learning applications in soil science. The research highlighted that lightweight architectures, multi-task learning, and transfer learning are emerging trends capable of improving model performance. It also identified significant obstacles, including data imbalance, restricted datasets, and inadequate model interpretability, which hinder wider implementation. It also discusses about different dataset as shown in Figure 10. The evaluation concluded that subsequent research must emphasize enhanced datasets, rigorous feature extraction techniques, and interpretable deep learning models to facilitate more efficient soil identification (Gyasi and Purushotham 2023).

Pandiri et al. (2024) claimed in this study, 96 samples were collected from agriculture fields in two ecological regions of Andhra Pradesh: (i) The Godavari River coastal zone, known for its alluvial and sandy soils suitable for paddy cultivation, and (ii) drought-prone areas with sandy and rocky soil ideal for vegetables. As in Figure 11, samples were taken from a depth of 5 cm to 10 cm at specific coordinates and categorized into 392 samples. Soil composition was analyzed using hydrometer and sieve methods under the supervision of the Department of Civil Engineering at MITS, with results plotted on the USDA



Figure 11. Soil image database (Kiran Pandiri, Murugan, and Goel 2024).

soil texture triangle. Images of 32 samples were captured using a 48-megapixel Samsung smartphone camera after removing organic materials and drying the soil at 100 for 24 hours. A styrofoam chamber was constructed to facilitate low-light imaging, ensuring accurate colour representation. These images were augmented to create the Indian regions soil image database, which is publicly available (Kiran Pandiri, Murugan, and Goel 2024).

6. Soil classification methods leveraging image processing and computer vision technologies

Computer vision and image processing technologies are used in soil classification problems. The traditional soil categorization has been revolutionized by recent developments in image processing and computer vision as shown in Figure 12, which allow for quick and non-invasive examination of the texture, colour, and the structure of soil. These methods provide scalable, reasonably priced options for environmental monitoring and precision farming. Table 2 summarizes the various image processing and computer vision techniques for soil categorization efficiency.

6.1. Methods utilized textural characteristics

(1971) investigated the reddish-brown basaltic soils of the malwa plateau in India, which highlighted several key factors responsible for their colour development. Through the application of multiple regression correlation analysis, a connection was established between the Munsell colour parameters of these soils and their chemical characteristics. The findings indicate that titanium and ferrous iron play crucial roles in determining the soil's 'hue'. Meanwhile, the 'value' aspect of the soil colour is significantly affected by the

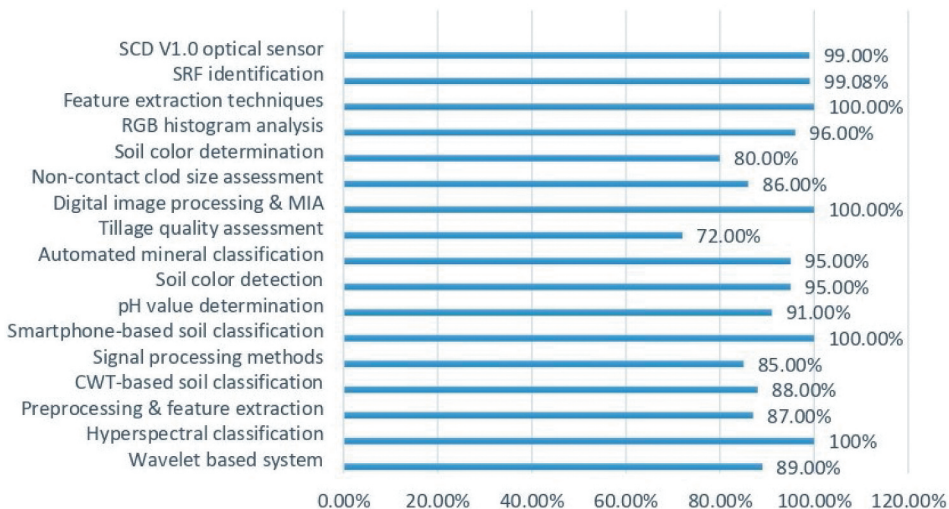


Figure 12. Accuracy of different models using image processing.

levels of clay and organic matter present. To evaluate the individual contributions of these factors to soil colour, a partial regression analysis was performed, allowing for a clearer understanding of their relative importance (Krishna Murti and Satyanarayana 1971).

Zhang, Younan, and King (2003) introduced a novel wavelet-based system for automating soil texture identification. Utilizing the wavelet transform for feature extraction captures both local and global textural information effectively. Implementation of a maximum likelihood classifier were trained on sample data and ML parameters were leveraged for optimal estimation results. Additionally, Fisher's linear discriminant analysis has been integrated to refine feature vector dimensionality, enhancing efficiency and accuracy. The system was tested on three soil texture classes: sand, silt, and clay. The final results confirm the wavelet-based approach's effectiveness in distinguishing these types, advancing automated soil classification techniques, and supporting precision agriculture, environmental monitoring, and geotechnical engineering (Zhang, Younan, and King 2003).

Zhang, Younan, and O'Hara (2005) proposed a novel system for automated soil texture classification that leverages hyperspectral soil signatures and wavelet-based statistical models. Hyperspectral data provide rich information and intrinsic properties about soil texture, offering a more comprehensive representation compared to traditional image-based methods. The designed framework integrates two probabilistic models in the wavelet domain for the recognition task; i.e. the maximum likelihood model and the hidden Markov model (HMM). These models are designed to effectively capture the underlying statistical characteristics of the hyperspectral soil signatures, enabling reliable and robust classification. The experimental result demonstrates the effectiveness of the proposed wavelet-based statistical models in accurately classifying soil textures using hyperspectral signatures. The HMM classifier in the 3-class method gives accuracies of 100%, 97%, 89%, 97%, and 100% for sand, silt, and sand dominant textures, respectively (Zhang, Younan, and O'Hara 2005).

Sofou, Evangelopoulos, and Maragos (2005) represented a sophisticated integration of modern computer vision methods for image feature extraction, texture analysis, and segmentation into consistent zones, highly pertinent to soil fine-scale morphology. The recommended framework incorporates a clustering approach based on a morphological partial differential equation and analyzes surface texture by representing image fluctuations as a local adjustment factor by utilizing both contrast and surface pattern data, utilizing multiscale image blurring. The study presents a combined image partitioning method that facilitates deeper analyses of soil images and feature extraction (Sofou, Evangelopoulos, and Maragos 2005).

Another method introduced by Breul et al. (2006) for comprehensive soil characterization using the image recorded by the innovative system. Recognizing the potential of texture analysis, which relies on global image analysis, the researchers have explored various techniques to extract meaningful insights from the acquired data. This method is designed to effectively characterize a high proportion of 80 μ m fine-grained materials and quickly distinguish them from coarse materials. This research investigates the influence of different factors, including particle size distribution, mineral composition, water content, and consolidation, on the progression of this phase, provides more profound insight of the complex connection within the soil matrix (Breul and Gourves 2006).

Botelho et al. (2006) introduced a method in which the determination of soil colour can be effectively achieved through visual comparison with Munsell charts, which relate closely to the presence of iron oxides and organic matter. However, instrument-based colour measurement via remote sensing offers enhanced precision due to its objective and controlled conditions. This research aimed to compare soil colours from Rio Grande do Sul, Brazil, using both Munsell charts and colorimetry, while correlating these colours with soil characteristics. The findings revealed minimal variability in chroma. Correlation coefficients indicates a strong alignment between measurements from the Munsell chart and the colorimeter, which proved to be an effective tool for quantifying colour, mitigating the psychophysical errors associated with visual assessments (Botelho et al. 2006).

Shenbagavalli and Ramar (2011) introduced an approach with a series of preprocessing steps, including grey-level thresholding, low-pass filtering, and edge enhancement, followed by feature extraction using a 3×3 Law's mask convolution. To construct the feature vector of soil images for subsequent operations; various parameters were calculated, such as, mean absolute value, mean, skewness, kurtosis, and statistical dispersion. The experimental results, conducted on a diverse set of soil textures, demonstrate the performance and impact of the proposed methods, highlighting the potential of this approach for automated soil classification (Shenbagavalli and Ramar 2011).

Chung et al. (2012) introduced an approach including an in-situ classification system and image processing techniques. The study investigated the potential of using RGB histograms to classify soil textures, analysing samples from major Korean paddy soil series. The analysis revealed linear patterns between silt content and histogram variables, such as brightness and the difference between the mode value and brightness. When the 5% averaged silt content was regressed with the 'mode-brightness' feature, the results showed high accuracy, with a squared correlation coefficient of 0.96 and low errors. Furthermore, the image processing technique constructs similar classification outcomes as the laboratory method for 48% of the samples (Chung et al. 2012).

Honawad et al. (2017) introduced the application of signal processing methods, including low mask, Gabor filter, and colour quantization, to enhance original soil images and extract valuable texture features for retrieval. The results, based on the datasets of 100 soil images belonging to 10 different types, demonstrated the effectiveness of the proposed method in achieving efficient retrieval performance and superior classification rates (Honawad et al. 2017).

Sudarsan et al. (2018) developed continuous wavelet transform (CWT) based computer vision algorithm to assess soil particle sizes from digital images captured with a low-cost portable microscope (5MP, $200 \times$ magnification). A total of 123 soil samples were gathered from two agricultural fields (Field26 and Field86), and three images were captured of air-dried, ground samples (2 mm), along with triplicate in-situ images from Field86. The images were converted to grayscale, and CWT was applied to analyse particle size variations. Further, two fractions were calculated: 'coarse' (2.0 mm to 0.5 mm) for sand, and 'fine' (less than 0.05 mm) for silt and clay, respectively. Strong correlations were found with laboratory measurement, achieving 87% and 88% prediction accuracy for coarse and fine fractions in Field26, and similar results for Field86. The wavelet algorithm shows promise as an effective proximal soil sensor. However, in-situ images yielded weaker predictions (48% for coarse and 56% for fine) due to field conditions, necessitating further research (Sudarsan et al. 2018).

Firman Ghazali et al. (2020) integrated field survey and lab data with Landsat 8 satellite imagery to predict soil moisture, salinity, and pH in agricultural fields. Water and salt content were measured using the SMI and SSI, while bare soil and paddy leaf models were utilized to create the soil pH index. After 30 days, a multi-temporal investigation spanning three dates revealed low salt levels and increasing soil moisture, with pH values ranging from 4.49 to 7.59. In contrast, to substantial connections in certain bare soil locations ($R^2 = 81.94\%$) and perfect correlations in paddy areas using the paddy leaf model ($R^2 = 100\%$), the bare soil model usually displayed poorer correlations between pH and moisture ($R^2 = 8.37\%$). The study emphasizes that when employing remote sensing, crop cover and soil conditions have a significant impact on the link between soil moisture, salinity and pH (Firman Ghazali et al. 2020).

Silvero et al. (2021) evaluated the effect of satellite spatial, spectral, and temporal resolutions on soil property mapping in southeastern Brazil (182 ha study site, Rafard, São Paulo State). A total of 162 soil samples were collected at 0–20 cm depth using a 100×100 m grid. Laboratory analyses included: clay and sand content (pipette method), organic matter (Walkley – Black oxidation), total iron (Fe_2O_3 via sulfuric acid digestion), and soil reflectance spectra (350–2500 nm using a FieldSpec Pro). Soil color (hue, value, chroma) was derived from Munsell notation. Three satellites were used: Landsat 8 operational land image OLI (30 m, 6 bands), Sentinel-2 multispectral instrument (MSI) (10–20 m, 6 bands), and PlanetScope (3 m, 4 bands). In addition to single-date imagery, multi-temporal composites (2016–2019) were generated: 45 Landsat 8 OLI images and 63 Sentinel-2 MSI images. Synthetic soil images were created using the GeoSpatial soil sensing system, which masks vegetation, water and clouds, and aggregates bare soil pixels by median reflectance.

Soil properties (clay, sand, OM, Fe_2O_3 , soil color) were predicted using the Cubist regression model with 4 bands (VIS – NIR) or 6 bands (VIS – NIR – SWIR) as predictors. Validation was performed using 10-fold cross-validation with 120 samples for training and 42 for testing. Model accuracy was evaluated using the coefficient of determination (R^2), RMSE, and mean absolute error (MAE):

$$R^2 = 1 - \frac{\sum_{i=1}^n (y_i - \hat{y}_i)^2}{\sum_{i=1}^n (y_i - \bar{y})^2}, \text{RMSE} = \sqrt{\frac{1}{n} \sum_{i=1}^n (y_i - \hat{y}_i)^2}, \quad \text{MAE} = \frac{1}{n} \sum_{i=1}^n |y_i - \hat{y}_i|$$

where, n is the number of samples; y_i is the measured soil property; \hat{y}_i is the predicted soil property; and \bar{y} is the mean value of the measured soil property. Sentinel-2 MSI synthetic soil image (SYSI) imagery achieved the highest performance ($R^2 = 0.48\text{--}0.78$). PlanetScope (3 m, 4 bands) did not improve predictions due to the absence of SWIR bands, but performed better for soil color ($R^2 > 0.5$). Landsat 8 OLI had shown lower predictive ability compared to Sentinel-2 MSI. Multi-temporal SYSI images consistently outperformed single-date imagery, capturing spectral patterns more strongly related to soil. Predicted clay content varied with resolution, with PlanetScope overestimating Cambisol values (270 g/kg) compared to Landsat SYSI (136 g/kg). Multi-temporal Sentinel-2 MSI synthetic soil index imagery provided the most accurate soil property predictions. The results indicate that temporal and spectral resolutions are more critical than spatial resolution for reliable soil mapping applications (Silvero et al. 2021).

6.2. Techniques with colour elements

Utilizing colour features from soil images offers a promising approach to enhance classification accuracy. The distinct colour characteristics of soil can provide insights into its composition, texture, and moisture levels. By analysing these colour features, researchers can effectively differentiate between various soil types. Recent developments in image processing techniques allow for the extraction and quantification of colour information, enabling more precise classification models. This approach not only streamlines the soil analysis process but also supports the integration of diverse data sources, leading to improved decision-making in soil management. Overall, leveraging colour features in soil classification presents a significant advancement in understanding and managing soil resources effectively.

Another development by O'Donnell et al. (2010) introduced a new method for identifying and quantifying soil redoximorphic features (SRF) from soil cores using a digital camera and image classification software. It also examined the impact of soil moisture and image processing on SRF interpretation. Eighteen soil horizons from chosen landscapes in the central claypan area of north-central missouri were captured under regulated lighting conditions. A 20 cm^2 area was analyzed for SRF quantification after determining the initial gravimetric water content. The overall accuracy for color determination based on Munsell soil color grouping was 99.60%. Rewetting air-dry horizon faces with 1 ml of deionized water showed minimal changes in determined SRF's after 7 applications, with mean changes of 2% (SD + 4) for low chroma and 0.03% (SD + 0.3) for high chroma SRFs between the seventh and tenth sequences. Interestingly, ten of the eighteen horizons exhibited an increased region of diminished chroma following ten rewetting cycles in contrast to their initial moisture state (O'Donnell et al. 2010).

Han et al. (2016) introduced a novel, low-cost, smartphone-based miniaturized sensor for soil colour classification was developed after analysing the contributions of machine vision and the observable wavelength range in soil classification. While the system's design for soil classification is straightforward and affordable, managing ambient light and machine parameters remains challenging. The highest identification accuracy achieved was 100% for yellow soil and burozem soil (Han et al. 2016).

Pethkar et al. (2018) developed various feature extraction techniques, including colour moments, HSV (hue, saturation, value), wavelet transforms, and Gabor filters, to analyse original soil images and extract their texture features for classification purposes. Categorization was performed using SVM classifier. Additionally, it determined that the SVM could be substituted with an artificial neural network (ANN) for classification tasks. The findings indicate that the proposed methodology effectively classifies soil types, achieving an overall accuracy of 100% (Pethkar 2018).

Gurubasava et al. (2018) employed a method utilizing digital image processing techniques has been proposed to determine and analyse the pH value of agricultural soil. The pH level indicates the degree of acidity or alkalinity, which significantly influences plant growth. The proposed system extracts key features in the form of RGB index values and calculates the mean values through PCA. During the testing phase, images are classified using PCA, and the index measurements are evaluated against the trained value to derive the final pH. The system achieved an accuracy of 100% for trained images and 91% for untrained images. Soil colour significantly influences agricultural practices, reflecting

attributes such as mineral content and organic matter. while the MSCC is commonly used for soil classification, it can be challenging to apply effectively (Gurubasava and Mahantesh 2018).

Hakim et al. (2025) introduced a unique technique by combining optical sensor technology with the RGB colour index, which is compared to the MSCC, soil colour detector version 1.0 (SCD V1.0) was created to improve soil colour identification efficiency and accuracy. The method was thoroughly tested on variety of soil types, including chernozems (Mollisols) at FH Erfurt, Germany, and ultisols (Baregbeg), inceptisols (Cilembu), and andisols (Lembang) in Indonesia. To evaluate SCD V1.0's accuracy and reliability, paired t-tests and analysis of variance were used to compare its results to the MSCC manual method and MetaVue VS3200 spectrophotometric analysis. With 100% soil color name identification accuracy and 99% colour index accuracy, the results were impressive. RMSE research showed that SCD V1.0 had smaller deviations (0.6–0.9) than MetaVue VS3200 and higher deviations (0.9–1.2) than MSCC, demonstrating the optical-based classification method's superior precision. The repeatability assessment indicated lower standard deviations for SCD V1.0 (0.10–0.15) than MSCC (0.25–0.32), indicating higher consistency. The agreement coefficient across all soil orders was 0.85, confirming the system's reliability. These findings demonstrate that SCD V1.0 is a reliable and automated soil colour detection approach that reduces human error and environmental variability. In tropical and subtropical locations, this technology has major implications for soil classification investigations, land survey and appraisal, and digital soil mapping. SCD V1.0 advances soil science and land management by delivering a precise, efficient and reproducible solution (Hakim 2025).

6.3. Techniques with other tools

Beyond soil colour and texture-based approaches, researchers have explored a wide range of alternative techniques for soil image analysis. Methods such as mean weight diameter estimation, tillage quality assessment, regression models, RF, RMSE-based evaluations, and hyperspectral imaging have shown strong potential, often delivering more accurate and reliable results.

The process of gathering, managing, and sieving soil samples to analyse soil clump measurement proliferation can be time-intensive, labour-demanding, and expensive. Bogrekci et al. (2007) developed a computer vision-based technique for non-contact measurement of soil tilth and clod size distribution, as an alternative to traditional mechanical sieving. Field experiments were carried out at Cranfield University, Silsoe, United Kingdom, on sandy loam soil (83% sand, 9% silt, 8% clay). Three soil tilths were prepared: (i) mouldboard plough (coarse tilth), (ii) mouldboard plough + chisel tine (intermediate tilth), and (iii) mouldboard plough + power harrow (fine tilth). Air-dried soil samples were mechanically sieved using sieve sizes ranging from 2.5 mm to 120 mm. The clod size distribution was expressed using the mean weight diameter (MWD):

$$D_{MW} = \sum_{i=0}^n \bar{x}_i \times w_i,$$

where, D_{MW} is the diameter of a clod/aggregate in mm; n is the number of sieves; \bar{x}_i is the mean diameter of a size fraction and w_i its weight fraction. Soil images were acquired using a Canon MV1 camcorder (4,50,000 pixels, progressive scan charge couple device) from 1.1 m above the soil surface. Both ambient and structured lighting conditions were tested. Images were geo-corrected with 40 ground control points using ERDAS imagine 8.3.1, followed by linear contrast stretching. Three image-processing methods were evaluated such as: edge detection (Sobel filter), contrast detection (grey-level thresholding) and aggregate finding and classification (AFC). A virtual sieve program was developed to classify soil aggregates into size fractions and compute grading curves and MWD. The effective clod diameter was derived from image features as:

$$d = 4 \times \frac{A}{P_c},$$

where, d is the diameter of a clod/aggregate in m; A is the clod area and P_c its perimeter. Image-based results were compared with sieve-derived values. The prediction accuracy was quantified using RMSE:

$$E_{RMS} = \sqrt{\frac{1}{n} \sum_{i=0}^n (x_i - y_i)^2},$$

where, n is the number of observations; E_{RMS} is the root-mean-square error; x_i are sieve-derived and y_i image-derived MWD values. Among the tested methods, contrast detection performed best with $RMSE = 14$ mm, followed by edge detection (21 mm) and AFC (37 mm). Image-based methods slightly overestimated clod size relative to sieving, mainly due to clod breakage during mechanical sieving and masking of small clods by larger aggregates. Regression analysis between image and sieve derived MWD showed a strong correlation ($R^2 = 0.96$), with image-based estimates approximately 21% higher. The proposed vision-based method proved to be a fast, non-contact, and repeatable tool for soil tilth assessment. Contrast detection was identified as the most reliable technique, providing a suitable alternative to mechanical sieving (Bogrekci and Godwin 2007).

Tillage operations use more than half of the energy in mechanized agriculture. Measuring tillage quality in real time can help adjust tillage tools, making ploughing more efficient and cost-effective. Ajdadi et al. (2016) developed an algorithm for real-time tillage quality assessment using image processing concepts. Images were captured at three distinct camera elevations, capturing nine sizes of soil agglomerates. Four techniques were employed to compute textural characteristics from the pictures: initial statistical computation, grey-tone spatial dependence matrix, grey level run length matrix, and texture binary encoding method. For feature selection, a data mining approach named CfsSubsetEval was applied. The best classification results came from neural networks with architectures of 19–19-1, 14–22-1, and 17–20-01 neurons for heights of 60 cm, 80 cm, and 100 cm, respectively. The highest accuracy for the ANN classifier was 72.04% for images taken at 60 cm. The method also effectively estimated the MWD of soil aggregates up to about 35 mm, achieving over 80% accuracy (Ajdadi et al. 2016).

Mapping the geographic dispersion of soil categories is crucial for efficient soil conservation and utilization. Shukla et al. (2018) evaluated the performance of the RF model for soil classification in various Indian districts. Environmental covariates, referred to as

'scorpan', were chosen to optimize the RF model for 11 distinct soil categories. A total of 35 digital layers were created using satellite data (including ALOS, Landsat-8, MODIS NDVI, RISAT-1, and Sentinel-1A) and climatic data (precipitation and temperature) to represent these covariates. The best RF parameters were identified based on the highest Cohen's kappa coefficient (K) and the fewest random split variables. Model evaluation focused on mapping accuracy, sensitivity to dataset size, and noise. For comparison, two other ML methods; namely, CART and CEB were also tested. Noise was added to the training set by assigning false classes, allowing for an assessment of model robustness. Performance measures included marginal rates, F-measure, Jaccard's coefficient, classification success index, and agreement coefficients to rank the algorithm. The RF model showed high stability against dataset reduction, with a significant accuracy drop only after a 60% reduction, while CEB and CART showed notable declines after 45% and 26%, respectively. There is increasing interest in automating the segmentation of landscapes into soil spatial entities to replace traditional, expensive manual techniques for soil categorization. Geographic object-based image analysis (GEOBIA) partitions remote sensing images or digital elevation models into consistent image units (Shukla et al. 2018).

Dornik et al. (2018) introduced an object-based approach to accurately delineate and to categorize soil types, employed digital representation of terrain and vegetation as auxiliary variables, along with the RF classification algorithm. Researchers compared the outcome of object-based categorization with that derived from a pixel-based approach using the similar classifier. Elevation incorporated 18 derivatives of the digital elevation model and five remote sensing indicators associated with vegetation and soil. By utilizing data from 171 soil profiles and along with their corresponding ecological variables, the RF technique pinpointed the most influential factors for soil type differentiation. A multi-resolution segmentation algorithm was applied to a stack of raster geo datasets based on these predictors, creating homogeneous objects that matched soil types, which were then classified using RF. Authors also performed categorization based on individual pixel using the same algorithm and soil observation, verifying both techniques with 30% of the soil observation. The findings revealed that GEOBIA was highly efficient in mapping soil types, attaining an overall accuracy of 58%, which was 10% greater than the refined pixel-level classification (Dornik, Drăgut, and Urdea 2018).

Accurate soil profile information is crucial for site characterization, mapping, and studies on soil formation and landscape modelling. Zhang et al. (2019) used digital soil mapping techniques to analyse 90 cm deep and 100 cm wide alfisol profile. Geochemical data were collected at 10 cm intervals, and digital images at a resolution of 1 cm^2 were used to predict various soil properties. Fuzzy c-means clustering was utilized for the profile and colour maps, and a confusion matrix was computed. The colour data points showed strong associations with SOC and silt content, and weathering parameters. RF models using the RGB color model had lower prediction accuracy for SOC ($R^2 = 0.57$, root mean square error (RMSE) = 2.41) compared to those using the CIE $L^*a^*b^*$ ($R^2 = 0.84$, RMSE = 1.57) and HSV ($R^2 = 0.84$, RMSE = 1.57) and HSV ($R^2 = 0.85$, RMSE = 1.46) models. The color and profile maps closely corresponded with the soil horizons identified in the field. Clusters formed on soil characteristics and weathering parameters were consistent with these horizons, demonstrating high overall accuracy ($p = 0.85$ and 0.86). The confusion matrix

indicated that horizon boundaries were undulating and slightly uneven (Zhang and Hartemink 2019).

Dyson et al. (2019) introduced one of the main challenges in precision agriculture is accurate crop–soil separation. In many AI-based methods, indices like the normalized difference vegetation index (NDVI), which serve as natural filters to lower training complexity and enhance deep learning performance, are derived from multispectral or hyperspectral data from Italy. One study produced a corrected radiometric index by applying a directional mathematical filter on high-resolution digital surface model (DSM) data, which improved NDVI segmentation. A compact CNN was used to process and down sample this index, which was created from pictures with roughly 3500×4500 pixels. The significance of integrating spectral indices with elevation data for precision agriculture was demonstrated by the results, which revealed that applying the DSM filter to NDVI prior to CNN classification increased vegetation – soil separation accuracy by up to 65% (Dyson et al. 2019).

Celik et al. (2022) emphasized that soil moisture is a key parameter for evaluating water resources, particularly in agriculture under global warming pressures. Leveraging recent advances in satellite remote sensing and deep learning, this study integrated high-spatial-resolution Sentinel-1 backscatter data with high-temporal-resolution SMAP observations to produce short-term, field-scale SM predictions. An LSTM-based deep learning model, using both static (topography, soil texture) and dynamic (SMAP SM, Sentinel-1 backscatter and ratios, climate data) features, was trained on in situ measurements from the International soil moisture network. The optimized model achieved high accuracy ($R^2 = 0.87$, RMSE = 0.046, unbiased RMSE = 0.045, MAE = 0.033). Performance declined in areas with high NDVI but improved in arid and semi-arid climates. The results demonstrate that daily soil moisture estimation from microwave remote sensing and geophysical data can be effectively achieved with LSTM, supporting applications in hydrology and agriculture (Furkan Celik et al. 2022).

Bouanani et al. (2025) noted that despite increasing pressure on agricultural systems from Africa's rapidly growing population, crop yields remain far below their potential, primarily because of poor soil quality. Increasing production requires efficient management of soil fertility, which is influenced by elements such as SOC, nutrient levels (N, P, and K), moisture content, and texture. An analysis of research conducted between 2008 and 2024 evaluated the application of AI techniques with publicly accessible hyperspectral satellite data (such as PRISMA and EnMAP) for mapping soil properties in Africa. Results indicate that AI, especially deep learning, has great promise, high-resolution hyperspectral sensors have been used infrequently, and their combined application is yet completely unexplored (El Bouanani et al. 2025).

Lou et al. (2025) highlighted that despite rapid advances in remote sensing, the classification of remains a crucial yet challenging task. Due to the inherent constraints of hyperspectral imaging, improving the accuracy and efficiency of hyperspectral images classification continues to be a central and widely discussed research concern. This review centres on a significant application domain of HSI classification – land use/land cover (LULC) mapping and is structured around four key objectives. Firstly, it provides a systematic overview of LULC classification using hyperspectral imagery, outlining its background and major challenges. Secondly, it compiles and evaluates a range of datasets tailored for LULC hyperspectral classification, serving as a valuable reference for

researchers. Thirdly, it examines both conventional machine learning approaches and state-of-the-art techniques, with particular emphasis on deep learning and spectral decomposition methods. Finally, it offers a comprehensive outlook on future directions in hyperspectral images classification, identifying pressing research gaps and emerging challenges. This review aims to serve as a foundational resource, guiding researchers through the current state and future potential of hyperspectral image classification (Lou et al. 2025).

7. Machine learning and deep learning models

ML and DL techniques, when combined with image processing, have opened new directions for soil classification. By automatically extracting meaningful patterns and features from soil images, these approaches enhance accuracy and efficiency compared to conventional methods. Table 3 outlines the various ML and DL techniques for soil classification and mapping.

ANNs are advanced machine learning frameworks designed based on the structure and function of the human brain. They consist of interconnected artificial neurons that work together to process information and perform calculations, as shown in Figure 13. ANNs excel in adapting and learning from large datasets, enabling them to handle complex non-linear systems. These networks are versatile, used for tasks like regression analysis, classification, and predicting future behaviours, as well as aiding in decision-making. Each neuron connects to others with weighted connections that influence the prediction. During training, ANNs optimize these weights by mapping inputs to outputs, allowing them to align their responses with the target system effectively. This self-training capability makes ANNs powerful tools for modelling and predicting complex behaviours.

Neural networks are structured with an entry layer, one or multiple intermediate layers and a result layer. The quantity of entry and result nodes varies based on the particular

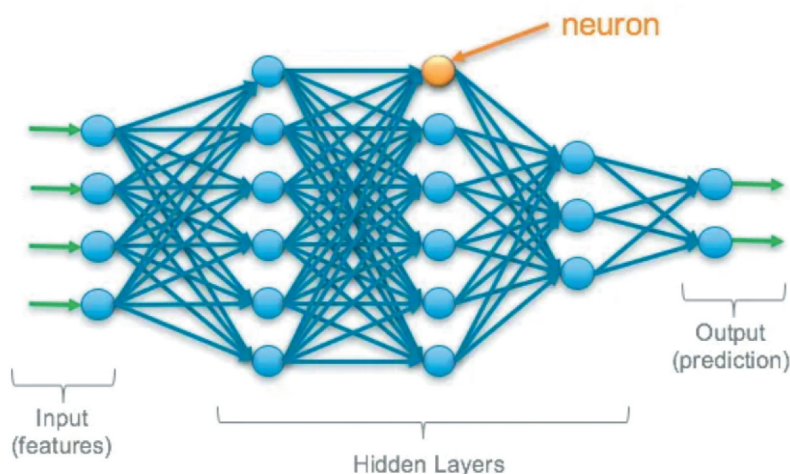


Figure 13. Schematic representation of deep learning (Ronaghan 2025).

issue being tackled. However, determining the suitable number of hidden neurons is less straightforward and needs to be evaluated for each case (Ronaghan 2025).

Pal (2005) has shown significant improvements in land cover classification accuracy by aggregating predictions through majority voting using ensemble method RF, which works on decision trees. A comparative study using Landsat enhanced thematic mapper plus data from United Kingdom, covering seven land cover classes, evaluated RF against SVM in terms of classification accuracy changing from 88.37% to 88.02% when the datasets increase, however overfitting has been controlled. Results indicated that RF outperformed over to SVM, while requiring fewer user-defined parameters to make it easier to implement. Also, RF classifier requires two parameters whereas the SVM require a number of user-defined parameters. These findings proves that RF act as an efficient and robust alternative for land cover classification tasks (Pal 2005).

Reale et al. (2018) categorized soils based on shared properties that affect their engineering behaviour under load. Accurately classifying sit conditions is essential for construction projects, but it can be costly and time-consuming as well. This study introduced an automated approach for classifying fine-textured soils utilizing a feed-forward ANN and cone penetration test (CPT) measurement, significantly reducing time and costs. Using 216 pairs of laboratory outcomes and CPT tests from five locations in Northern Croatia, the ANN models were trained and validated. The models were further tested with CPT data from the Veliki Vrh landslide, achieving nearly 90% accuracy in predicting classifications according to the European soil classification system and the unified soil classification system (USCS). The model outperformed over previously published standard model in correlation coefficient, average error, and classification accuracy. The study confirms relationships between CPT results, fine particle percentage, liquid limit, and plasticity index, suggesting that as the dataset grows, soil classification will become cheaper, faster and less labour-intensive (Reale et al. 2018).

Compressive spectral imaging systems hold great potential for object classification, but traditional methods for soil classification often struggle due to the trade-off between invariance and variability among soil types. Yu et al. (2019) investigated a system utilizing a liquid crystal tunable filter along with a proposed 3D-CNN for soil categorization. First obtain soil compaction assessment using a detector with low spatial resolution, and then rebuild hyperspectral images with improved geo-spatial and wavelength precision using a compressive sensing technique. Unlike traditional wavelength-driven categorization techniques that extract features separately, this method employed PCA for dimensionality reduction in the feature space. Additionally, also introduce a variant perception framework for adaptable feature extraction, ultimately leading to a 3D-CNN for soil categorization (Yu et al. 2019).

In the realm of artificial intelligence, DL algorithms excel at learning from unstructured data such as text, sound, images, and videos. Unlike traditional machine learning, which focuses on labelling and detecting meaningful patterns, deep learning automates feature extraction directly from the data. This branch of AI aims to empower machines to perform tasks skilfully using intelligent software. Deep learning models, often based on artificial neural networks, can have hundreds of hidden layers, with no upper limit on the number of layers. Each layer performs non-linear functions in parallel, processing the output from the previous layer and passing it to the next. While increasing the number of layers enhances network complexity, deep neural networks operate without human

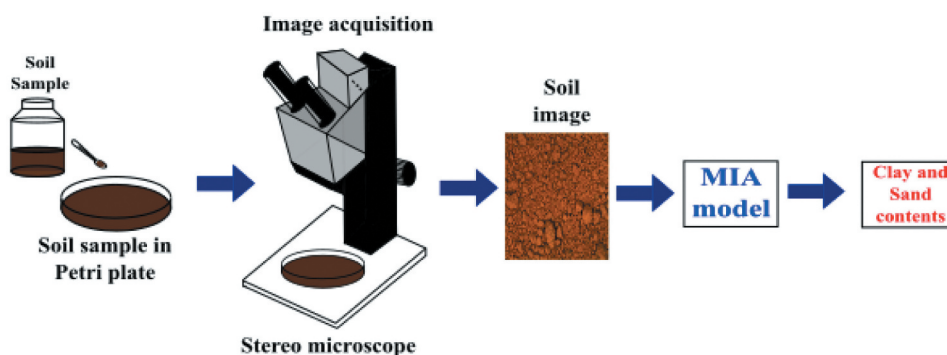


Figure 14. Image-based method for clay and sand content estimates (de Oliveira Morais et al. 2019).

intervention, learning directly from the data provided. To achieve optimal performance, it is essential to supply adequate and relevant input data. Although various types of 3D images can be used, stereo images are particularly effective as they extract 3D information being impacted by lighting variations.

Morais et al. (2019) developed a digital image analysis framework for soil texture prediction using MIA as shown in Figure 14. A total of 63 topsoil samples (0–10 cm, 500 g each) were collected from five municipalities across three Brazilian states (Goiás, Pernambuco, and Mato Grosso). Samples were dried at 45° C for 48 h, ground, sieved (< 2 mm), and analyzed for sand, clay, and silt fractions using the standard pipette method as reference. Subsamples (2 g) were imaged using a Leica EZ4 D stereo microscope with digital camera (2048 × 1536 px, RGB TIFF format). Images were transformed into RGB, HSV, and grayscale color spaces. Segmentation removed shadows and non-soil regions. Feature extraction generated seven color data matrices (RGB, HSV, grayscale, and their combinations), yielding 200–1500 variables per image. Partial least squares regression was applied to correlate image features with sand and clay contents. The dataset was split into calibration (45 samples) and validation (18 samples) using the Kennard – Stone algorithm, and also evaluated with bootstrap resampling (1,000 iterations). There is a very significant correlation $R^2 > 0.92$ Within the range of 25–75% for both sand and clay, this demonstrates the good linear agreement between the suggested approach and the conventional method. A multivariate regression model is deemed excellent if its RPD value falls between 2.5 and 3.0 $RPD > 3$, For MIA models that use Grayscale, HSV, and fused data (RGB+HSV and RGB+HSV+Grayscale), RPD values greater than 3.0 are regarded as excellent. This indicates that the HSV+Grayscale combination alone is not appropriate for determining the amount of clay. Sand estimate shows similar patterns. Texture classification accuracy was 100%, as MIA-predicted USDA classes matched pipette-based references for all 18 validation samples. This lab trial showed that traditional soil texture analysis (pipette method) takes (104 h for 25 samples), while the MIA method delivers results in just ~ 10 minutes after sample preparation. MIA reduces analysis time by ~ 50 h, cost < 90% of the standard method, and can handle four times more samples per batch. Thus, it is faster, cheaper, and more efficient (de Oliveira Morais et al. 2019).

Singh et al. (2019) focused on quantifying soil properties from hyperspectral data obtained from land use/land cover area frame survey (LUCAS) using LSTM network-based deep learning model. Additionally, PCA is applied to the LUCAS datasets to reduce

dimensionality, enhancing the calibration of the LSTMs. The proposed framework achieves impressive results, with the highest R^2 of 0.94 for organic carbon. Its effectiveness is demonstrated through comparisons with existing models, including PLSR, SVR, PCR, MLR and SWR (Singh and Kasana 2019).

Gyasi et al. (2023) introduced a transformative approach in soil classification, leveraging neural network with multiple hidden layers to improve analytical capabilities. This methodology facilitates the automatic extraction of complex soil features from raw datasets, minimizing the necessity for manual feature extraction. CNNs have proven particularly effective in categorizing soil types based on remote. Various deep-learning architectures have significantly impacted the field, establishing themselves as widely recognized benchmarks. Prominent examples include Alexnet, GoogleNet, ResNet, and VGG-16 which serve as essential key constituent in various soil categorization systems. In this section, delve into several key deep learning techniques, including ML, CNNs and transfer learning, that are employed for the classification and identification of different soil types (Gyasi and Purushotham 2023). Padmapriya et al. (2023) evaluated the soil classification model's performance, metrics such as accuracy, precision, loss, recall and F1-score are employed as shown in Figure 23. Accuracy represents the ratio of correctly predicted samples to total samples. Recall indicates the ratio of actual positive predictions to available positive samples, while precision (positive predictive value) is the ratio of true positives to predicted positives. The F1-score is the harmonic mean of precision and recall (Padmapriya and Sasilatha 2023).

Bhat et al. (2023) developed a GBRT-based deep learning surrogate model, with optimized Bayesian optimization, for precise crop selection based on soil characteristics. The system achieves an exceptional F1-score of 1.0 across all classes and an average classification accuracy of 100%, ensuring highly accurate crop recommendation. Explainable AI (XAI) further evaluates the impact of input parameters, enhancing the model interpretability and reliability (Bhat, Hussain, and Huang 2023).

Accurate soil property prediction is vital for sustainable land management and the provision of agriculture. Liu et al. (2024) presented an CNN-LSTM-Attention model that integrates temporal and spatial feature extraction with attention mechanism, utilizing the LUCAS soil dataset to estimate key properties like organic carbon (OC), nitrogen (N), calcium carbonate (CaCO_3), and pH. The LSTM acquires chronological pattern, whereas the CNN identifies spatial characteristics and the attention mechanism emphasizes the essential information as demonstrated in Figure 15. The working of the LSTM model is explained using the following equations:

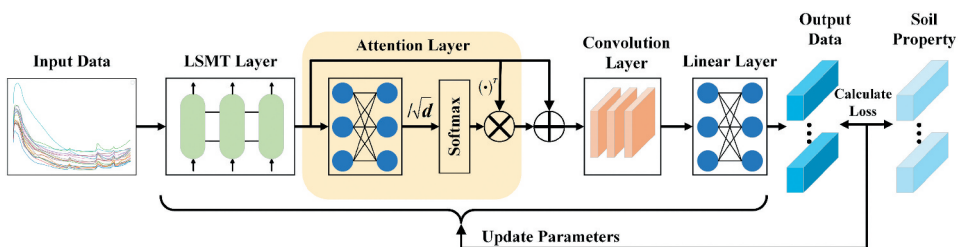


Figure 15. The framework of the proposed LSTM-CNN-attention model (Y. Liu et al. 2024).

$$f_t = \sigma(W_f \cdot [h_{t-1}, x_t] + b_f)$$

$$i_t = \sigma(W_i \cdot [h_{t-1}, x_t] + b_i)$$

$$\tilde{C}_t = \tanh(W_C \cdot [h_{t-1}, x_t] + b_C)$$

$$C_t = f_t \times C_{t-1} + i_t \times \tilde{C}_t$$

$$o_t = \sigma(W_o \cdot [h_{t-1}, x_t] + b_o)$$

$$h_t = o_t \times \tanh(C_t)$$

Here, the LSTM model regulates information flow through three gates: the forget gate (f_t), input gate (i_t), and output gate (o_t); σ and \tanh denote the sigmoid and hyperbolic tangent activation functions, respectively, while W and b represent the weight matrix and bias term; intermediate cell state and the long-term cell state are denoted by \tilde{C}_t and C_t , respectively. Finally, $t - 1$ and t refer to the previous and current time steps; and x_t and h_t denote the input and output at the current time step. This gated mechanism enables the network to capture long-term dependencies and overcome vanishing gradient issues in standard RNNs. The model achieves impressive performance, with R^2 values of 0.949 (OC), 0.916 (N), 0.943 (CaCO_3), and 0.926 (pH), and corresponding RPD values of 3.940, 3.737, 5.377 and 3.352. These findings surpass those achieved by conventional models (PLSR, SVR, RF) and deep learning models (CNN-LSTM, Gated recurrent unit), demonstrating superior performance over S-AlexNet in recognizing time-based and geometric attributes. This underscores the model's capability to improve the precision and dependability of soil property estimations (Y. Liu et al. 2024).

Gupta et al. (2024) classified the report presented in Figure 16 highlighted the effectiveness of our developed deep learning model in categorizing various soil types. The model attained a weighted mean classification efficiency, recall and F1-score of 0.74, demonstrating a strong and well-balanced assessment across all soil categories. Notably, it demonstrated strong identification capabilities for black soil and clay soil, with F1-scores

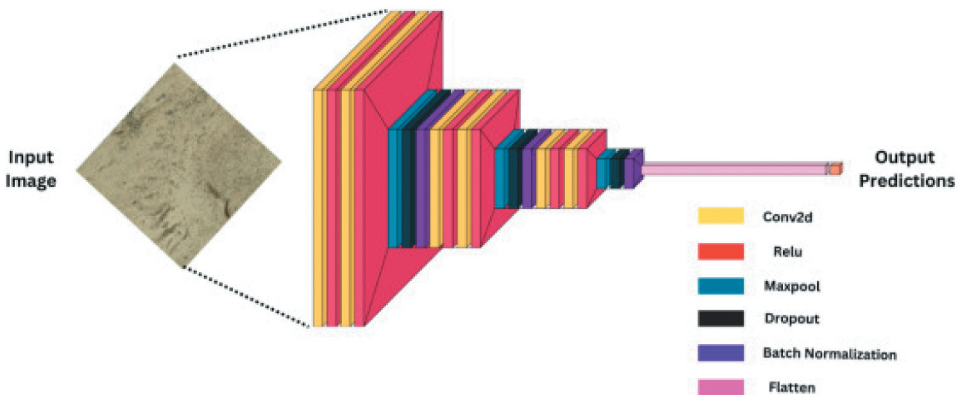


Figure 16. Hyperspectral soil classification architecture (Gupta et al. 2024).

of 0.83 and 0.86, respectively. These outcomes illustrated the model's recall to distinct soil types. However, the F1-scores of 0.55 for red soil and 0.53 for alluvial soil indicate areas where improvement is needed. With an overall test set accuracy of 0.74, the model reflects significant generalization potential. Throughout 50 epochs, the suggested soil categorization model surpassed traditional methods. Proposed model attained superior accuracy compared to Logistic Regression, GRU, LSTM, RNN, and SVM. The loss comparisons further validated its efficiency, as the suggested model exhibited faster convergence and the lowest loss, whereas other models shown slower convergence and elevated error rates. The findings underscore the enhanced precision and resilience of the suggested methodology (Gupta et al. 2024).

Pandiri et al. (2024) extracted features to classify soil types through fully connected and softmax layers. The proposed soilNet network was tested on 334 images of five soil classes as shown in Figure 13, achieving an overall efficiency of 97.20%. The light-soilnet network processed these images ($728 \times 728 \times 1$) in 11 seconds. It provides essential metrics such as TP, TN, FP, FN, precision, recall and F1-score, which were used to evaluate the proposed framework and performance was compared with findings from various research ().

Hemdan et al. (2024) proposed an IOT-based hybrid CNN-SVM model for classifying five soil types, achieving superior accuracy with AlexNet-SVM 96%, ResNet50-SVM 95%, and SqueezeNet-SVM 86% compared to standalone CNN models (Hemdan and Al-Atroush 2024).

El-Rawy et al. (2024) revealed that high soil salinity in the Siwa Oasis, Egypt, negatively impacts agriculture despite its economic significance. This research proposes a method combining remote sensing and modified U-Net (MU-NET) deep learning framework to identify and delineate regions affected by salinity and vegetation. The MU-NET design incorporates a dual-tier nested U-configuration combined with a residual U-block to enhance segmentation accuracy. We utilized 91 Landsat 8 satellite images collected over ten years, featuring 11 spectral bands at 30 m resolution, and validated the model with field survey data. Findings indicate a rise in soil salinity, particularly in spatial distribution, correlating with accelerated salt accumulation and plant cover decline. The model attained superior efficiency, with accuracies of 91.27% for salinity and 90.83% for vegetation, outperforming existing methods in the literature (El-Rawy et al. 2024).

The methodology for assessing soil characteristics via visible and near-infrared spectral analysis has progressed in parallel with the deep learning frameworks. Ke et al. (2024)

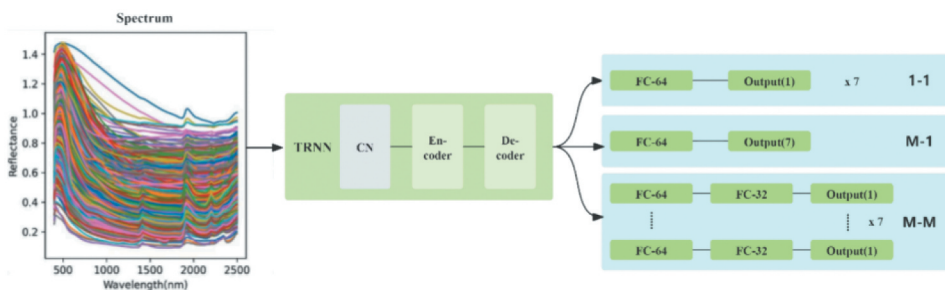


Figure 17. Three output structures for TRNN: TRNN 1-1, TRNN M-1, and TRNN M-M (Ke, Ren, and Yin 2024).

leverage the LUCAS soil spectral library to investigate the effectiveness of encoder-decoder architecture in enhancing CNN regression predictions. By combining an encoder-decoder architecture into a six-layer CNN framework (TRNN), substantially improved the performance of superficial CNNs for predicting seven soil properties as illustrated in Figure 17. The utilized methods like integrate gradients, deepLift, gradientshap and deepLiftshap to interpret the TRNN frameworks outputs. A framework based on unprocessed spectra obtained high accuracy, surpassing residual architectures, LSTMs, various CNN designs, and conventional machine learning methods from prior studies. Also, examined the effects of multi-task (TRNN 1-M and TRNN M-M) versus single-task (TRNN 1-1) output structures on performance, finding that multi-task structures reduced efficacy. The TRNN model achieved impressive regression results for the selected soil characteristics such as cation exchange capacity, organic carbon content, calcium carbonate content, pH value, clay, silt, and sand composition with R^2 values outstripping 0.93 for all (Ke, Ren, and Yin 2024).

Saberioon et al. (2024) focused on predicting SOC, a key factor in climate change and greenhouse gas emission, by leveraging soil spectral libraries. The study evaluates the effectiveness of two DL algorithms: 1D CNN and a fully connected neural network (FCNN) with stacked autoencoder (SAE) trait identification, using data from the LUCAS database. SAE was employed to extract high-level features from the visible-near-infrared-shortwave infrared spectra of 11,441 soil samples, which served as inputs for the 1DCNN and FCNN models as shown in Figure 18. The SAE-DL models outperformed those using the complete spectra and a RF framework for comparison. The finest outcomes were obtained with the SAE-1D CNN model, yielding an R^2 of 0.78 and RMSE of 3.94%, demonstrating the superiority of the 1D CNN over FCNN (Saberioon et al. 2024). Additionally, macro average metrics further underscore the model's balanced performance, with accuracy and recall both around 0.70. These findings validate the effectiveness of this approach for soil type classification in geospace informatics, thereby supporting informed decision-making for extraterrestrial missions.

In the world of multimodal fusion, an innovative approach for integrating diverse data types for predictive tasks has been underexplored in geotechnical engineering. Guo et al. (2025) classified excavated soils quickly and accurately using a soil

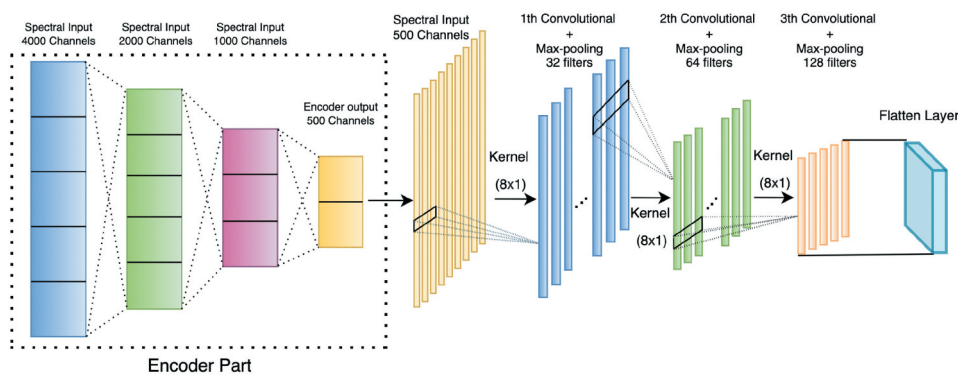


Figure 18. Stacked autoencoder architecture (Saberioon et al. 2024).

information collection system at China's largest soil transfer platform. Authors generated 3,243 groups of diverse data, including soil images, cone index curves, TDR waveform time series, and discrete net weight measurements along with descriptive textual data on soil structure. Following data expansion, compile an extensive dataset consisting of 23,122 labelled records, depending on the USCS, moisture content, and mineral constituents. To train multimodal deep learning models, multiple fusion approaches were implemented including seven early fusion, three transitional fusion and two late fusion techniques, respectively. The model's effectiveness was evaluated through various evaluation metrics, including loss, accuracy, F1-score, precision, recall, specificity, negative predictive value, false positive rate, and area under the receiver operating characteristic curve. The findings demonstrated that intermediate fusion approaches outperformed late fusion, with the two-stage transitional fusion strategy incorporating five modalities accomplishing the maximum precision, surpassing 0.99 on the test dataset. This multimodal fusion approach effectively uncovers correlations among diverse soil data, offering significant scientific and engineering insights in geotechnics (Q.-M. Guo et al. 2025).

Zhao et al. (2025) specified a deep cement mixing (DCM) technology, which plays a crucial role in geotechnical engineering, particularly for enhancing ground conditions in soft soil foundation. Accurate soil layer classification is vital for optimizing DCM effectiveness and maintaining structural integrity. Nevertheless, a disparity in soil layer data frequently leads to the insufficient representation of specific soil types, potentially diminishing categorization precision and model dependability. To overcome this disadvantage, an adaptive boundary-synthetic minority over-sampling technique. (AB-SMOTE) technique was implemented that improves the conventional sample expansion technique by dynamically broadening the minority class zones and determining the refined subzones for synthesizing representative examples. Furthermore, developed a particle swarm optimization-enhanced RF (PSO-RF) model to enhance soil layer categorization, enriching broad applicability and controlled model complexity. Computational analysis outcomes indicate that the AB-SMOTE algorithm efficiently addresses irregular data distribution by synthesizing high-fidelity data, substantially improving model training. Implementing the PSO-RF model on the proportionate dataset leads to notable enhancements in categorization, precision, and recall. The study validated an improved soil layer classification framework for DCM, combining AB-SMOTE with PSO-RF. Five construction parameters were used as features: current (I), energy consumption (E), penetration speed (v), water admixture (w), and depth (d). Minority soil classes (sand and clay) were augmented using AB-SMOTE, which generates synthetic samples in clean minority subregions:

$$AB - SMOTE(A, S_{\min}, S_{\max}, z),$$

where, S_{\min} and S_{\max} denote minority and majority classes, A is the set of assistant seeds, and z is the number of synthetic samples. Soil layers were identified using a PSO-optimized RF. Particle updates followed:

$$V_i^{k+1} = \omega V_i^k + c_1 r_1 (P_i^k - X_i^k) + c_2 r_2 (P_g^k - X_i^k)$$

$$X_i^{k+1} = X_i^k + V_i^{k+1}$$

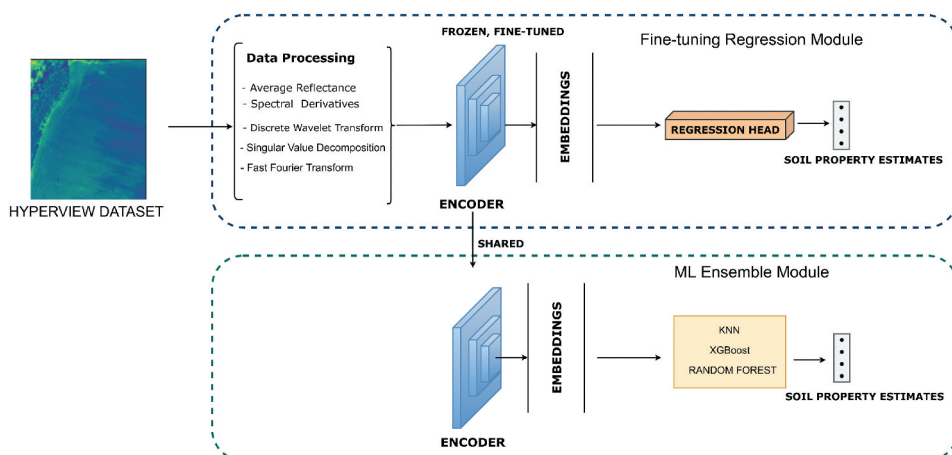


Figure 19. Architecture of the proposed HyperSoilNet framework (La'ah Ayuba et al. 2025).

where, c_1 represents the cognitive learning factor, c_2 represents the social learning factor, ω is the inertia weight, and r_1, r_2 are random numbers uniformly chosen between 0 and 1. The symbol k indicates the current iteration, i refers to the i th particle, P_i is the best position found so far by particle i , and P_g is the best position found among all particles (Y. Zhao and Teng 2025).

Ayuba et al. (2025) employed a HyperSoilNet model as shown in Figure 19, which is a hybrid deep learning framework designed to estimate soil properties from hyperspectral imagery by combining a pretrained hyperspectral-specific CNN backbone with an optimized ensembled machine learning concepts. The hyperview challenge dataset for potassium oxide, phosphorus pentoxide, magnesium, and soil pH prediction was evaluated, the framework achieved a leaderboard score of 0.762, outperforming state-of-the-art methods. Ablation studies and spectral analysis demonstrated that integrating deep representation learning with traditional ML techniques enhances feature extraction and prediction accuracy, highlighting HyperSoilNet's potential for advancing precision agriculture and sustainable soil management (La'ah Ayuba et al. 2025).

7.1. Establishing a model for soil type classification

This infrastructure for training a soil classification model depends on the chosen model, its complexity, and the dataset's type and size. After selecting a model, its architecture must be designed, which includes defining the layer count, input image size, filter counts and sizes, activation functions, neuron counts per layer, and overall structure. It is essential to verify the output shape and the count of learnable parameters by executing a framework architecture overview. Training DL framework requires a robust CPU, ideally a multicore with a clock speed of at least 2 GHz. While using a GPU is not essential, but it is advised for quicker training, with NVIDIA GPUs being a common choice. The RAM requirement varies with datasets size and model complexity, but a minimum of 16GB is advisable. Additionally, ample storage (SSD or HDD) is necessary for large datasets, and a dependable power source is crucial to avoid interruptions during training. Software

requirements include GPU drivers and libraries like compute unified device architecture (CUDA) and CUDA-deep neural network (Chetlur et al. 2014), if GPU is used. Python is the primary programming language for DL supported by frameworks such as TensorFlow, Keras, Caffe, and PyTorch, which simplify model building and training. Google Colab offers an alternative infrastructure for deep learning but requires a high-bandwidth internet for efficient datasets and framework downloads. Since the target implementation for soil identification is edge devices like smartphones, which lack high-performance processors, it is wise to train the model on a standard machine. Once the infrastructure is set, the model can be validated with soil image samples to understand the features extracted by its convolutional layers. The datasets should be divided into three parts: training set, validation set for hyperparameter tuning, and test set for evaluation. Deep learning models, often seen as black boxes, comprise multiple layers that convert input data in complex ways, making feature extraction challenging to interpret. Activation maps from convolutional layers help identify features recognized from specific soil images. Each feature map is a 2D array representing outputs from the convolutional filters, with weights learned through back propagation. As data passes through the network, each layer captures increasingly complex features, enhancing the model's capability.

7.2. Evaluation of deep learning model's effectiveness through training process

The deep learning model designed for recognizing and delineating key soil horizons were trained over 500 epochs, with the optimized framework stored once synchronization. Training performance graphs for the A, B and C horizons were plotted to evaluate framework efficiency during the training phase [Figure 18](#). The loss curves for both training and validation datasets showed a significant decrease from epochs 30 to 100, followed by a plateau from 100 to 500 epochs. Similarly, pixel accuracy (PA) curves exhibited a sharp increase during the first 100 epochs and then stabilized. The flattening of loss and PA curves indicated that the model converged with optimal hyperparameter suitable for identifying and delineating soil horizons. For the A horizon, the model achieved a minimum loss of 0.11 and a maximum PA of 0.89 in the training datasets, while the validation dataset reached a minimum loss of 0.16 and a maximum PA of 0.85. The B horizon resulted in a minimum training loss of 0.18 and a maximum PA of 0.83, with validation metrics showing a minimum loss of 0.26 and a maximum PA of 0.78. For the C horizon, the training dataset recorded a minimum loss of 0.15 and a maximum PA of 0.86, whereas the validation had a minimum loss of 0.20 and a maximum PA of 0.80. Overall, the results indicated that DL model performed best in identifying and delineating the A horizon, followed by the B and C horizon, respectively (Jiang et al. 2021).

For model training, a learning rate of 0.01 was established, with validation occurring every 30 iterations. SoilNet model was trained over 8 iterations, with each epoch consisting of 12 iterations. During this process, the convolutional and pooling layers automatically extracted texture features from the soil images, and the network's weights were updated iteratively. [Figure 20](#) contains four graphs that compare the performance of a model trained to classify three different soil horizons, A, B, and C. Each horizon (A, B and C) follows a different learning curve, suggesting that some layers might be easier or harder to classify. The top two graphs show how the loss decreases over time, while the bottom two graphs

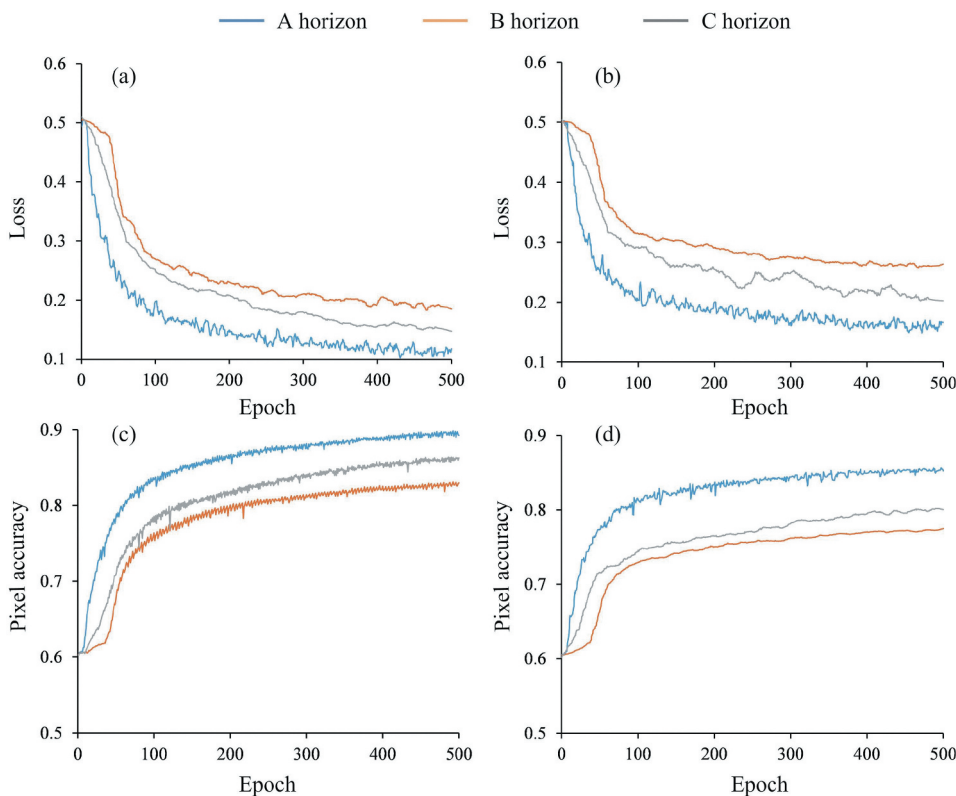


Figure 20. Loss comparison (Jiang et al. 2021).

illustrate how pixel accuracy improves as the model trains. Loss represents the prediction error, and a lower loss indicates better learning. Initially, the loss is high for all three soil horizons, but as training progresses, it gradually decreases, meaning the model is improving. Conversely, pixel accuracy, which measures how well the model classifies soil pixels, starts with lower values and increases with each epoch, indicating that the model is learning to make more accurate predictions. Overall, the SoilNet network achieved an impressive efficiency of 97.20% in classifying the five different soil types. Additionally, the Light-SoilNet network required 11 seconds to test 334 soil images, each sized at $728 \times 728 \times 1$ pixels. The training progress of the proposed framework is depicted in Figure 20.

8. Metrics for performance assessment

The assessment of the model's efficiency depends on several key metrics: precision, recall, F1-score, and accuracy. The mathematical formulas of these metrics are shown in Table 4. This confusion matrix as shown in Figure 21 represents the performance of a soil classification model, where different soil types (clay, loam, loamy sand, sand, and sandy loam) are classified based on the target labels. The numbers in each cell indicate the count and percentage of predictions for each class. Green cells along the diagonal represent correctly classified samples, while red cells indicate misclassified instances. The percentages

Table 4. Model performance indicators.

Metric	Formula	Description
True Positives (TP)	$TP(i) = X_{ii}$	Number of correctly predicted positive instances.
False Negatives (FN)	$FN(i) = \sum_{j=1}^n X_{ij} - TP(i)$	Number of positive instances incorrectly classified as negative.
False Positives (FP)	$FP(i) = \sum_{j=1}^n X_{ji} - TP(i)$	Number of negative instances incorrectly classified as positive.
True Negatives (TN)	$TN(i) = \sum_{i=1}^n \sum_{j=1}^n X_{ij} - TP(i) - FP(i) - FN(i)$	Number of correctly predicted negative instances.
Precision (P)	$\frac{TP(i)}{TP(i) + FP(i)}$	Measures how many of the predicted positive instances are actually positive.
Recall (R)	$\frac{TP(i)}{TP(i) + FN(i)}$	Measures how well the model identifies actual positive instances (also known as Sensitivity).
F1-score	$\frac{2 \times P \times R}{P + R}$	Harmonic mean of precision and recall, balancing both metrics.
Accuracy	$\frac{TP(i) + TN(i)}{TP(i) + FP(i) + FN(i) + TN(i)}$	Proportion of correctly classified instances across all categories.

at the bottom show the accuracy and misclassification rate of each target class. The model performs well in most cases, achieving high accuracy for clay (100%), loam (90%), loamy sand (96%), and sandy loam (97.20%). However, it struggles slightly with sand, showing an 88.50% accuracy and an 11.5% misclassification rate. Overall, the model demonstrates strong classification ability, but some errors occur in distinguishing similar soil types, particularly between loamy sand and sand (). The end accuracy is close to 90%, and the training process shows a steady rise in model accuracy over the course of subsequent epochs as shown in [Figure 22](#). While keeping this information, the training loss shows a steep drop in the first few repetitions and then stays low, suggesting quick convergence and steady learning. These findings imply that the model produces strong prediction performance by successfully capturing the underlying patterns in the data.

Many notable contributions are included in the performance comparison of different soil classification approaches as shown in [Table 5](#) and in graphical format as shown in [Figure 23](#). These performance metrics indicate that the proposed methodology demonstrated strong capabilities in accurately categorizing soil samples into the target categories, which suggested high accuracy, balanced precision, recall, and F1-score.

Padmapriya et al. (2023) evaluate the soil classification model's performance, metrics such as accuracy, precision, loss, recall, and F1-score are employed as illustrated in [Figure 23](#). Accuracy represents the ratio of correctly predicted samples to total samples. Recall indicates the ratio of actual positive predictions to available positive samples, while precision (positive predictive value) is the ratio of true positives to predicted positives. The F1-score is the harmonic mean of precision and recall (Padmapriya and Sasilatha 2023).

Bhat et al. (2023) developed a GBRT-based deep learning surrogate model, with optimized Bayesian optimization, for precise crop selection based on soil characteristics. The system achieves an exceptional F1-score of 1.0 across all classes and an average classification accuracy of 100%, ensuring highly accurate crop recommendation. XAI further evaluates the impact of input parameters, enhancing the model interpretability and reliability (Bhat, Hussain, and Huang 2023).



Figure 21. Confusion matrix (Kiran Pandiri, Murugan, and Goel 2024).

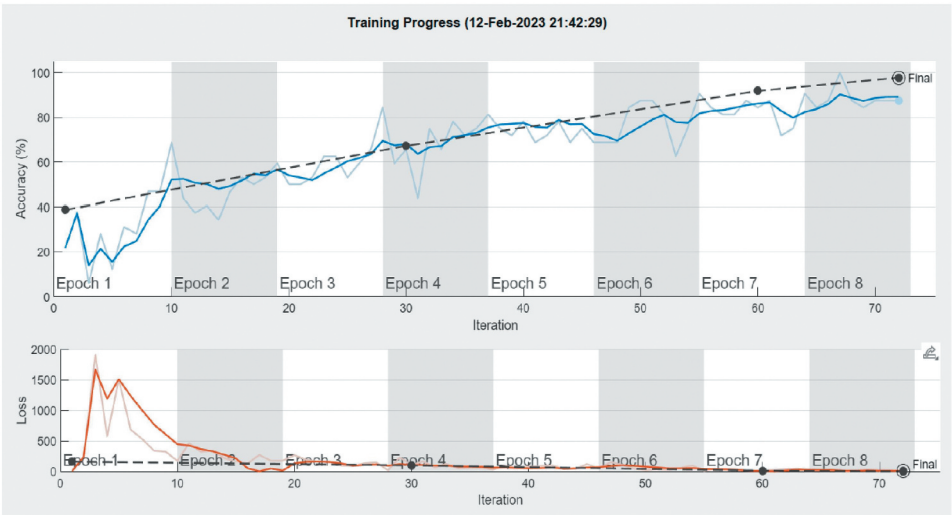


Figure 22. Training progress (Kiran Pandiri, Murugan, and Goel 2024).

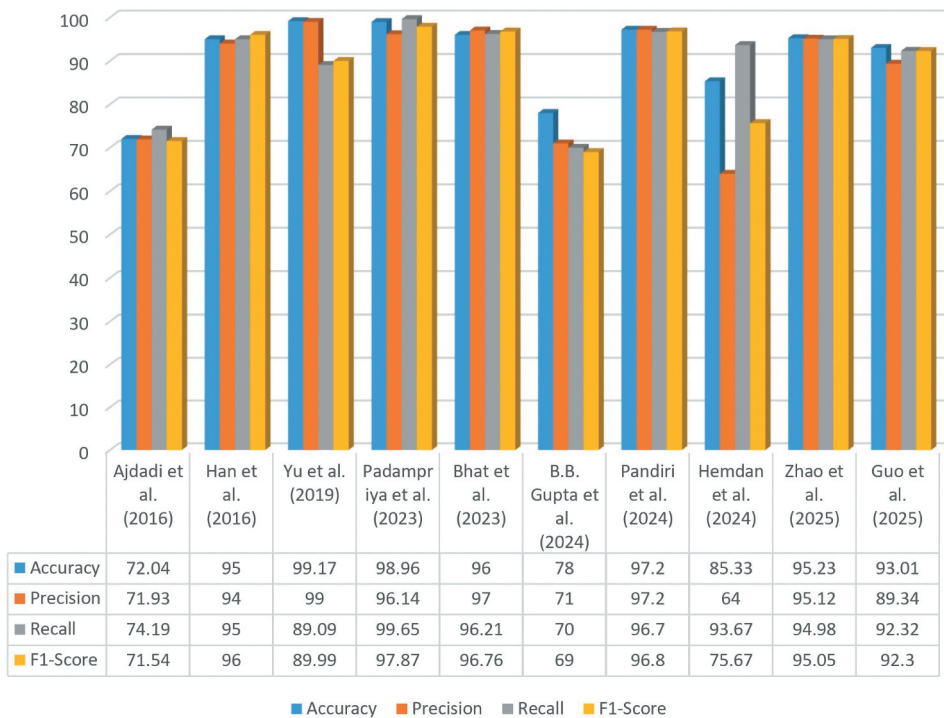


Figure 23. Performance comparison of different studies.

Table 5. Performance comparison of different studies based on detection results.

Authors	Data Size	Accuracy (%)	Precision (%)	Recall (%)	F1-score (%)
Ajdadi et al. (2016)	1350	72.04	71.93	74.19	71.54
Han et al. (2016)	500	95.00	94.00	95.00	96.00
Yu et al. (2019)	44,500	99.17	99.00	89.09	89.99
Padmapriya and Sasilatha (2023)	5938	98.96	96.14	99.65	97.87
Bhat, Hussain, and Huang (2023)	–	96.00	97.00	96.21	96.76
Gupta et al. (2024)	1555	74.00	70.00	69.00	69.00
Pandiri et al. (2024)	1960	97.20	97.20	96.70	96.80
Hemdan and Al-Atroush (2024)	252	85.33	64.00	93.67	75.67
Y. Zhao and Teng (2025)	–	95.23	95.12	94.98	95.05
H. Guo et al. (2025)	–	93.01	89.34	92.32	92.30

Pandiri et al. (2024) extracted features are used to classify soil types through fully connected and softmax layers. The proposed SoilNet network was tested on 334 images of five soil classes as shown in Figure 11, achieving an overall efficiency of 97.20%. The Light-SoilNet network processed these images ($728 \times 728 \times 1$) in 11 seconds. Figure 20 illustrates progress, while performance metrics were calculated from the confusion matrix generated during testing. It provides essential metrics such as TP, TN, FP, FN, precision, recall, and F1-score, which were used to evaluate the proposed framework, and its performance was compared with findings from various research Pandiri et al. (2024).

Hemdan et al. (2024) proposed an IOT-based hybrid CNN-SVM model for classifying five soil types, achieving superior accuracy with AlexNet-SVM 96%, ResNet50-SVM 95%, and SqueezeNet-SVM 86% compared to standalone CNN models (Hemdan and Al-Atroush 2024).

As the Figure 23 compares the reported performance metrics (accuracy, precision, recall, and F1-score) of various soil classification studies published between 2016 and 2025. Earlier methods, such as Ajdadi et al. (2016), which relied mainly on handcrafted features and shallow classifiers, achieved relatively modest accuracy ($\approx 72\%$) and lower recall/F1-scores, reflecting the limitations of traditional machine learning in handling soil texture variability. Similarly, Gupta et al. (2024) reported only $\approx 78\%$ accuracy, which can be attributed to a smaller dataset size and less robust feature representation. In contrast, more recent works leveraging deep learning, feature fusion, and advanced imaging techniques (Yu et al., 2019; Padampiriya et al., 2023; Pandiri et al., 2024; Zhao et al., 2025) consistently outperform earlier studies, with performance values exceeding 95% across all metrics. Notably, Yu et al. (2019), using a 3D-CNN with compressive spectral imaging, and Padampiriya et al. (2023), applying multi-feature fusion, achieved near-perfect results ($\approx 99\%$) accuracy, recall, and F1-score).

The contribution of spectral and hyperspectral imaging has been particularly significant, as these methods capture both spatial and spectral information across a wide range of wavelengths, enabling fine discrimination of soil texture and mineral composition. Similarly, remote sensing techniques have broadened the applicability of soil classification by providing large-scale, non-invasive data acquisition, linking laboratory-level precision with field-scale monitoring. Overall, the figure highlights a clear upward trend in performance over time, showing how advancements in deep learning, spectral/hyperspectral

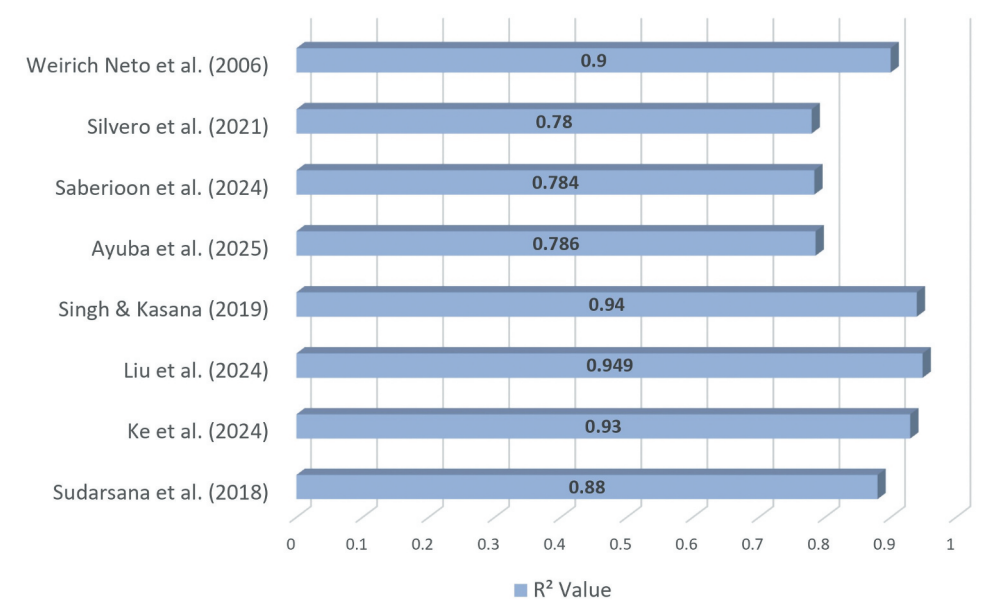


Figure 24. Performance comparison of different regression studies.

imaging, and remote sensing technologies have transformed soil classification from modest reliability in early models to highly accurate and robust systems in recent years.

As Figure 24 presents a comparative analysis of R^2 values reported in regression-based soil prediction studies. Among these, Liu et al. (2024) ($R^2 = 0.949$) and Singh & Kasana (2019) ($R^2 = 0.94$) demonstrated the strongest predictive ability, indicating highly reliable regression models for soil parameter estimation. Similarly, Ke et al. (2024) also achieved a high R^2 of 0.93, while Weirich Neto et al. (2006) and Sudarsana et al. (2018) reported values of 0.90 and 0.88, respectively, showing robust though slightly less powerful performance. On the other hand, studies such as Silvero et al. (2021) ($R^2 = 0.78$), Saberioon et al. (2024) ($R^2 = 0.784$), and Ayuba et al. (2025) ($R^2 = 0.786$) achieved comparatively lower values, suggesting moderate predictive capability that may be attributed to smaller datasets, greater soil variability, or less advanced modelling techniques. Overall, the figure highlights that while early regression approaches demonstrated useful accuracy ($R^2 \approx 0.88\text{--}0.90$), more recent studies integrating advanced regression frameworks and machine learning enhancements have pushed performance closer to $R^2 \approx 0.95$, reflecting a clear improvement in soil property prediction reliability over time.

9. Conclusion

Soil classification is a vital process that impacts numerous aspects of society, from agriculture and land use to environmental protection and climate change mitigation. The traditional technology for soil classification primarily involves field surveys, laboratory analysis, and expert assessment, which are very time-consuming, subjective, and may not capture the full variability of soils, especially in large or heterogeneous areas. This review has provided a comprehensive examination of soil classification, highlighting its fundamental principles, methodologies, and integration of cutting-edge technologies, including image analysis, computer vision with deep learning, and use of ViTs, which overcome the limitations of traditional methods. The key soil characteristics used by these systems include colour, texture, and particle size, intending to replace traditional manual soil inspections. This review presents an overview of various soil classification methodologies, categorizing them into two main groups: one is based on image processing and computer vision, which encompasses three essential steps: methods utilizing textural characteristics, techniques with colour elements, and techniques with other tools. Also shows the accuracy of different models using image processing. Then another group is soil classification using some deep learning and machine learning models. Moreover, deep learning demonstrated remarkable effectiveness in soil classification, as compared to the conventional manual technique, deep learning-based soil classification achieves higher accuracy and efficiency. These models can quickly analyse the vast amount of soil images and identify intricate patterns that may be challenging for human experts to identify accurately. Additionally, this paper analyzes various databases created by researchers, remarking those factors like the gap between the soil surface and cameras, along with atmospheric and lightning conditions, are critical for effective soil classification.

10. Challenges

Research on soil categorization has advanced significantly, but there are still a number of issues that need to be addressed. The generalizability of models is a significant drawback because the majority of methods are created and tested on datasets that are specific to a given location. Because soils with varying textures, mineral compositions, and environmental circumstances might not be correctly categorized by models trained elsewhere, this raises questions regarding cross-regional adaptation. The availability of sizable and varied datasets presents another difficulty; current research frequently uses small sample sizes, which limits the models' resilience and transferability. Another obstacle to widespread use is the complexity of processing hyperspectral data. Despite the excellent accuracy offered by advanced spectrum approaches, their applicability in actual agricultural settings is diminished by their dependence on complex preparation procedures and computationally demanding algorithms. Furthermore, few studies have addressed field-ready, user-friendly applications, and many approaches are still limited to controlled laboratory or experimental settings. Additionally, there are not enough long-term studies to test the stability and adaptability of soil classification techniques over time and in different environmental settings. Lastly, there is a lack of interdisciplinary cooperation in the sector; like soil science, computer vision, and machine learning frequently advance separately rather than together.

11. Future works

Future studies should concentrate on developing accurate, useful and straightforward solutions for farming situations. For wider usage, it will be crucial to create efficient techniques that are computationally efficient while maintaining the accuracy of sophisticated models. Without compromising performance, the incorporation of machine learning methods designed for massive soil datasets may expedite data processing and enhance usability. The resilience and adaptability of the model will be improved by gathering more, broader datasets that span a range of soil types and geographical areas. In order to make sure that classification techniques are trustworthy outside of localized settings, future research should also give priority to cross-validation across areas and soil properties. Building creative, reliable, and field-ready systems will require collaborative and interdisciplinary approaches that combine knowledge of soil science with developments in computer vision, remote sensing, and machine learning. Furthermore, to comprehend the temporal stability of these techniques and their adaptation to shifting soil and climatic circumstances, long-term monitoring studies are required.

Disclosure statement

No potential conflict of interest was reported by the author(s).

References

Ahmad, M. B. 2023. "Benefits and Drawbacks of Different Soil Types." *IPHO-Journal of Advance Research in Agriculture and Environmental Science* 1 (7): 01–08. <http://iphopen.org/index.php/aes/article/view/16>.

- Ajdadi, F. R., Y. A. Gilandeh, K. Mollazade, and R. P. Hasanazadeh. 2016. "Application of Machine Vision for Classification of Soil Aggregate Size." *Soil and Tillage Research* 162:8–17. <https://doi.org/10.1016/j.still.2016.04.012>.
- Aydemir, S., S. Keskin, and L. R. Drees. 2004. "Quantification of Soil Features Using Digital Image Processing (DIP) Techniques." *Geoderma* 119 (1–2): 1–8. [https://doi.org/10.1016/S0016-7061\(03\)00218-0](https://doi.org/10.1016/S0016-7061(03)00218-0).
- Aydn, Y., Ü. Iskdağ, G. Bekdas, S. M. Nigdeli, and Z. W. Geem. 2023. "Use of Machine Learning Techniques in Soil Classification." *Sustainability* 15 (3): 2374. <https://doi.org/10.3390/su15032374>.
- Azizi, A., Y. A. Gilandeh, T. Mesri-Gundoshmian, A. A. Saleh-Bigdeli, and H. A. Moghaddam. 2020. "Classification of Soil Aggregates: A Novel Approach Based on Deep Learning." *Soil and Tillage Research* 199:104586. <https://doi.org/10.1016/j.still.2020.104586>.
- Barman, U., and R. D. Choudhury. 2020. "Soil Texture Classification Using Multi Class Support Vector Machine." *Information Processing in Agriculture* 7 (2): 318–332. <https://doi.org/10.1016/j.inpa.2019.08.001>.
- Barman, U., R. Dev Choudhury, N. Talukdar, P. Deka, I. Kalita, and N. Rahman. 2018. "Predication of Soil pH Using HSI Colour Image Processing and Regression Over Guwahati, Assam, India." *Journal of Applied and Natural Science* 10 (2): 805–809. <https://doi.org/10.31018/jans.v10i2.1701>.
- Bhat, S. A., I. Hussain, and N.-F. Huang. 2023. "Soil Suitability Classification for Crop Selection in Precision Agriculture Using GBRT-Based Hybrid DNN Surrogate Models." *Ecological Informatics* 75:102109. <https://doi.org/10.1016/j.ecoinf.2023.102109>.
- Bogrecki, I., and R. J. Godwin. 2007. "Development of an Image-Processing Technique for Soil Tilth Sensing." *Biosystems Engineering* 97 (3): 323–331. <https://doi.org/10.1016/j.biosystemseng.2007.03.025>.
- Botelho, M. R., R. S. Diniz Dalmolin, F. de Araújo Pedron, A. C. de Azevedo, R. B. Rodrigues, and P. Miguel. 2006. "Color measurement in soils from rio grande do sul state with munsell charts and by colorimetry." *Ciência Rural* 36 (4): 1179–1185. <https://doi.org/10.1590/S0103-84782006000400021>.
- Bouslihim, Y., A. Rochdi, and N. E. A. Paaza. 2021. "Machine Learning Approaches for the Prediction of Soil Aggregate Stability." *Heliyon* 7 (3): 2021. <https://doi.org/10.1016/j.heliyon.2021.e06480>.
- Breul, P., and R. Gourves. 2006. "In Field Soil Characterization: Approach Based on Texture Image Analysis." *Journal of Geotechnical and Geoenvironmental Engineering* 132 (1): 102–107. [https://doi.org/10.1061/\(ASCE\)1090-0241\(2006\)132:1\(102\)](https://doi.org/10.1061/(ASCE)1090-0241(2006)132:1(102)).
- Carlomagno, A., G. Montanaro, G. Corigliano, and V. Nuzzo. 2024. "Soil Management Enhances Resilience in Marginal Areas by Preserving Soil Functions and Reducing Soil Loss." *InSpoke 7 Meeting_Contributions*. <https://hdl.handle.net/11563/191857>.
- Chetlur, S., C. Woolley, P. Vandermersch, J. Cohen, J. Tran, B. Catanzaro, and E. Shelhamer. 2014. "cudnn: Efficient Primitives for Deep Learning." *arXiv preprint arXiv:1410.0759*.
- Chung, S.-O., K.-H. Cho, J.-W. Cho, K.-Y. Jung, and T. Yamakawa. 2012. "Texture Classification Algorithm Using RGB Characteristics of Soil Images." *Journal of the Faculty of Agriculture, Kyushu University* 57 (2): 393–397. <https://doi.org/10.5109/25196>.
- de Oliveira Morais, P. A., D. M. de Souza, M. T. de Melo Carvalho, B. E. Madari, and A. E. de Oliveira. 2019. "Predicting Soil Texture Using Image Analysis." *Microchemical Journal* 146:455–463.
- Dornik, A., L. Drăgut, and P. Urdea. 2018. "Classification of Soil Types Using Geographic Object-Based Image Analysis and Random Forests." *Pedosphere* 28 (6): 913–925. [https://doi.org/10.1016/S1002-0160\(17\)60377-1](https://doi.org/10.1016/S1002-0160(17)60377-1).
- Dyson, J., A. Mancini, E. Frontoni, and P. Zingaretti. 2019. "Deep Learning for Soil and Crop Segmentation from Remotely Sensed Data." *Remote Sensing* 11 (16): 1859. <https://doi.org/10.3390/rs11161859>.
- El Bouanani, N., A. Laamrani, H. Hajji, M. Bourriz, F. Bourzeix, H. Ait Abdelali, A. El-Battay, A. Amazirh, and A. Chehbouni. 2025. "Estimating Soil Attributes for Yield Gap Reduction in Africa Using Hyperspectral Remote Sensing Data with Artificial Intelligence Methods: An Extensive Review and Synthesis." *Remote Sensing* 17 (9): 1597. <https://doi.org/10.3390/rs17091597>.
- El-Rawy, M., S. Y. Sayed, M. A. AbdelRahman, A. Makhloof, N. Al-Arifi, and M. Khaled Abd-Allah. 2024. "Assessing and Segmenting Salt-Affected Soils Using in-Situ Ec Measurements, Remote Sensing,

- and a Modified Deep Learning Mu-Net Convolutional Neural Network." *Ecological Informatics* 81:102652. <https://doi.org/10.1016/j.ecoinf.2024.102652>.
- Firman Ghazali, M., K. Wikantika, A. B. Harto, and A. Kondoh. 2020. "Generating Soil Salinity, Soil Moisture, Soil pH from Satellite Imagery and Its Analysis." *Information Processing in Agriculture* 7 (2): 294–306. <https://doi.org/10.1016/j.inpa.2019.08.003>.
- Furkan Celik, M., M. Serkan Isik, O. Yuzugullu, N. Fajraoui, and E. Erten. 2022. "Soil Moisture Prediction from Remote Sensing Images Coupled with Climate, Soil Texture and Topography via Deep Learning." *Remote Sensing* 14 (21): 5584. <https://doi.org/10.3390/rs14215584>.
- Guo, H., C. Zhang, H. Fang, T. Rabczuk, and X. Zhuang. 2025. "Deep Learning to Evaluate Seismic-Induced Soil Liquefaction and Modified Transfer Learning Between Various Data Sources." *Underground Space* 23:220–242.
- Guo, Q.-M., L.-T. Zhan, Z.-Y. Yin, H. Feng, G.-Q. Yang, Y.-M. Chen, and Y.-A. Chen. 2025. "Correlation of Excavated Soil Multi-Source Heterogeneous Data Using Multimodal Diffusion Model." *Acta Geotechnica* 20:4977–5005. <https://doi.org/10.1007/s11440-025-02690-z>.
- Gupta, B. B., A. Gaurav, V. Arya, and R. W. Attar. 2024. "Advance Deep Learning for Soil Type Classification in Space Informatics." *Journal of Industrial Information Integration* 42:100712. <https://doi.org/10.1016/j.jii.2024.100712>.
- Gurubasava, M. S., and S. D. Mahantesh. 2018. "Analysis of Agricultural Soil pH Using Digital Image Processing." *International Journal of Research in Advent Technology* 6 (8): 1812–1816.
- Gyasi, E. K., and S. Purushotham. 2023. "Advancements in Soil Classification: An In-Depth Analysis of Current Deep Learning Techniques and Emerging Trends." *Air, Soil and Water Research* 16:11786221231214069. <https://doi.org/10.1177/11786221231214069>.
- Hakim, D. L. 2025. "Optical Sensor-Based Soil Color Identification in Tropical and Subtropical Regions." *Malaysian Journal of Soil Science* 29:165–178.
- Han, P., D. Dong, X. Zhao, L. Jiao, and Y. Lang. 2016. "A Smartphone-Based Soil Color Sensor: For Soil Type Classification." *Computers and Electronics in Agriculture* 123:232–241. <https://doi.org/10.1016/j.compag.2016.02.024>.
- Hemdan, E. E.-D., and M. E. Al-Atroush. 2024. "An Efficient IoT-Based Soil Image Recognition System Using Hybrid Deep Learning for Smart Geotechnical and Geological Engineering Applications." *Multimedia Tools & Applications* 83 (25): 1–22. <https://doi.org/10.1007/s11042-024-18230-y>.
- Honawad, S. K., S. S. Chinchali, K. Pawar, and P. Deshpande. 2017. "Soil Classification and Suitable Crop Prediction." In *National Conference on Advances in Computational Biology, Communication, and Data Analytics, IOSR Journal of Computer Engineering (IOSR-JCE)*, 25–29.
- Htun, H. H., M. Biehl, and N. Petkov. 2023. "Survey of Feature Selection and Extraction Techniques for Stock Market Prediction." *Financial Innovation* 9 (1): 26. <https://doi.org/10.1186/s40854-022-00441-7>.
- Inazumi, S., S. Intui, A. Jotisankasa, S. Chaiprakaikeow, and K. Kojima. 2020. "Artificial Intelligence System for Supporting Soil Classification." *Results in Engineering* 8:100188. <https://doi.org/10.1016/j.rineng.2020.100188>.
- Jiang, Z.-D., P. R. Owens, C.-L. Zhang, K. R. Brye, D. C. Weindorf, K. Adhikari, Z.-X. Sun, F.-J. Sun, and Q.-B. Wang. 2021. "Towards a Dynamic Soil Survey: Identifying and Delineating Soil Horizons In-Situ Using Deep Learning." *Geoderma* 401:115341. <https://doi.org/10.1016/j.geoderma.2021.115341>.
- Ke, Z., S. Ren, and L. Yin. 2024. "Advancing Soil Property Prediction with Encoder-Decoder Structures Integrating Traditional Deep Learning Methods in vis-nir Spectroscopy." *Geoderma* 449:117006. <https://doi.org/10.1016/j.geoderma.2024.117006>.
- Kim, Y. I., W. H. Park, Y. Shin, J.-W. Park, B. Engel, Y.-J. Yun, and W. S. Jang. 2024. "Applications of Machine Learning and Remote Sensing in Soil and Water Conservation." *Hydrology* 11 (11): 183. <https://doi.org/10.3390/hydrology11110183>.
- Kiran Pandiri, D. N., R. Murugan, and T. Goel. 2024. "Smart Soil Image Classification System Using Lightweight Convolutional Neural Network." *Expert Systems with Applications* 238 (PD): 122185. <https://doi.org/10.1016/j.eswa.2023.122185>.

- Krishna Murti, G. S. R., and K. V. S. Satyanarayana. 1971. "Influence of Chemical Characteristics in the Development of Soil Colour." *Geoderma* 5 (3): 243–248. [https://doi.org/10.1016/0016-7061\(71\)90013-9](https://doi.org/10.1016/0016-7061(71)90013-9).
- Krizhevsky, A., I. Sutskever, and G. E. Hinton. 2012. "Imagenet Classification with Deep Convolutional Neural Networks." *Advances in Neural Information Processing Systems* 25.
- La'ah Ayuba, D., J.-Y. Guillemaut, B. Marti-Cardona, and O. Mendez. 2025. "A Hybrid Framework for Soil Property Estimation from Hyperspectral Imaging." *Remote Sensing* 17 (15): 2568. <https://doi.org/10.3390/rs17152568>.
- Lecun, Y., L. Bottou, Y. Bengio, and P. Haffner. 1998. "Gradient-Based Learning Applied to Document Recognition." *Proceedings of the IEEE* 86 (11): 2278–2324.
- Li, J., F. Goerlandt, and G. Reniers. 2021. "An Overview of Scientometric Mapping for the Safety Science Community: Methods, Tools, and Framework." *Safety Science* 134:105093. <https://doi.org/10.1016/j.ssci.2020.105093>.
- Liu, C.-Y., C.-Y. Ku, T.-Y. Wu, and Y.-C. Ku. 2024. "An Advanced Soil Classification Method Employing the Random Forest Technique in Machine Learning." *Applied Sciences* 14 (16): 7202. <https://doi.org/10.3390/app14167202>.
- Liu, Y., L. Shen, X. Zhu, Y. Xie, and S. He. 2024. "Spectral Data-Driven Prediction of Soil Properties Using LSTM-CNN-Attention Model." *Applied Sciences* 14 (24): 11687. <https://doi.org/10.3390/app142411687>.
- Lou, C., M. A. Al-Qaness, D. Al-Alimi, A. Dahou, M. A. Elaziz, L. Abualigah, and A. A. Ewees. 2025. "Land Use/Land Cover (LULC) Classification Using Hyperspectral Images: A Review." *Geo-Spatial Information Science* 28 (2): 345–386. <https://doi.org/10.1080/10095020.2024.2332638>.
- Maniyath, S. R., R. Hebbar, K. N. Akshatha, L. S. Architha, and S. Rama Subramoniam. 2018. "Soil Color Detection Using KNN Classifier." In *2018 International Conference on Design Innovations for 3Cs Compute Communicate Control (ICDI3C)*, Bangalore, India, 52–55. IEEE. <https://doi.org/10.1109/ICDI3C.2018.00019>.
- Moher, D., A. Liberati, J. Tetzlaff, D. G. Altman, and T. PRISMA Group*. 2009. "Preferred Reporting Items for Systematic Reviews and Meta-Analyses: The PRISMA Statement." *Annals of Internal Medicine* 151 (4): 264–269. <https://doi.org/10.7326/0003-4819-151-4-200908180-00135>.
- Neto, P. W., E. Borghi, C. Sverzut, E. Mantovani, R. Gomide, and W. Newes. 2006. "Multivariate Analysis of Soil Resistance to Penetration in No-Tillage." *Ciência Rural* 36:1186–1192. <https://doi.org/10.1590/S0103-84782006000400022>.
- O'Donnell, T. K., K. W. Goyne, R. J. Miles, C. Baffaut, S. H. Anderson, and K. A. Sudduth. 2010. "Identification and Quantification of Soil Redoximorphic Features by Digital Image Processing." *Geoderma* 157 (3–4): 86–96. <https://doi.org/10.1016/j.geoderma.2010.03.019>.
- Padmapriya, J., and T. Sasilatha. 2023. "Deep Learning Based Multi-Labelled Soil Classification and Empirical Estimation Toward Sustainable Agriculture." *Engineering Applications of Artificial Intelligence* 119:105690. <https://doi.org/10.1016/j.engappai.2022.105690>.
- Pal, M. 2005. "Random Forest Classifier for Remote Sensing Classification." *International Journal of Remote Sensing* 26 (1): 217–222. <https://doi.org/10.1080/01431160412331269698>.
- Pethkar, S. 2018. "Classification of Soil Image Using Feature Extraction." *International Journal for Research in Applied Science and Engineering Technology* 6 (7): 819–823. <https://doi.org/10.22214/ijraset.2018.7138>.
- Rahman, M. M., M. Kamruzzaman, S. Shahid, K. R. Thorp, H. Rahaman, M. M. Shahriyar, A. S. Islam, and M. D. Huda. 2023. "A GIS Framework to Demarcate Suitable Lands for Combine Harvesters Using Satellite DEM and Physical Properties of Soil." *Journal of Geovisualization and Spatial Analysis* 7 (2): 27. <https://doi.org/10.1007/s41651-023-00156-y>.
- Reale, C., K. Gavin, L. Librić, and D. Jurić-Kačunić. 2018. "Automatic Classification of Fine-Grained Soils Using Cpt Measurements and Artificial Neural Networks." *Advanced Engineering Informatics* 36:207–215. <https://doi.org/10.1016/j.aei.2018.04.003>.
- Ronaghan, S. 2025. "Deep Learning: Common Architectures — srnghn.medium.com." <https://srnghn.medium.com/deep-learning-common-architectures-6071d47cb383>.
- Saberioon, M., A. Gholizadeh, A. Ghaznavi, S. Chabrilat, and V. Khosravi. 2024. "Enhancing Soil Organic Carbon Prediction of LUCAS Soil Database Using Deep Learning and Deep Feature

- Selection." *Computers and Electronics in Agriculture* 227:109494. <https://doi.org/10.1016/j.compag.2024.109494>.
- Sarkar, T., and M. Mishra. 2018. "Soil Erosion Susceptibility Mapping with the Application of Logistic Regression and Artificial Neural Network." *Journal of Geovisualization and Spatial Analysis* 2 (1): 8. <https://doi.org/10.1007/s41651-018-0015-9>.
- Shenbagavalli, R., and K. Ramar. 2011. "Classification of Soil Textures Based on Laws Features Extracted from Preprocessing Images on Sequential and Random Windows." *Bonfring International Journal of Advances in Image Processing* 1 (1): 15. <https://doi.org/10.9756/BIJAIP.1004>.
- Shukla, G., R. D. Garg, H. Shanker Srivastava, and P. Kumar Garg. 2018. "An Effective Implementation and Assessment of a Random Forest Classifier as a Soil Spatial Predictive Model." *International Journal of Remote Sensing* 39 (8): 2637–2669. <https://doi.org/10.1080/01431161.2018.1430399>.
- Silvero, N. E., J. A. Dematte, J. de Souza Vieira, F. A. de Oliveira Mello, M. Taynara Accorsi Amorim, R. Roberto Poppiel, W. de Sousa Mendes, and B. R. Bonfatti. 2021. "Soil Property Maps with Satellite Images at Multiple Scales and Its Impact on Management and Classification." *Geoderma* 397:115089. <https://doi.org/10.1016/j.geoderma.2021.115089>.
- Singh, S., and S. S. Kasana. 2019. "Estimation of Soil Properties from the EU Spectral Library Using Long Short-Term Memory Networks." *Geoderma Regional* 18:e00233. <https://doi.org/10.1016/j.geodrs.2019.e00233>.
- Sofou, A., G. Evangelopoulos, and P. Maragos. 2005. "Soil Image Segmentation and Texture Analysis: A Computer Vision Approach." *IEEE Geoscience & Remote Sensing Letters* 2 (4): 394–398. <https://doi.org/10.1109/LGRS.2005.851752>.
- Srunitha, K., and S. Padmavathi. 2016. "Performance of SVM Classifier for Image Based Soil Classification." In *2016 International Conference on Signal Processing, Communication, Power and Embedded System (SCOPES)*, Paralakhemundi, India, 411–415. IEEE. <https://doi.org/10.1109/SCOPES.2016.7955863>.
- Sudarsan, B., W. Ji, V. Adamchuk, and A. Biswas. 2018. "Characterizing Soil Particle Sizes Using Wavelet Analysis of Microscope Images." *Computers and Electronics in Agriculture* 148:217–225. <https://doi.org/10.1016/j.compag.2018.03.019>.
- Sujatha, M., and C. D. Jaidhar. 2024. "Machine Learning-Based Approaches to Enhance the Soil Fertility—A Review." *Expert Systems with Applications* 240:122557. <https://doi.org/10.1016/j.eswa.2023.122557>.
- Tobiszewski, M., and C. Vakh. 2023. "Analytical Applications of Smartphones for Agricultural Soil Analysis." *Analytical & Bioanalytical Chemistry* 415 (18): 3703–3715. <https://doi.org/10.1007/s00216-023-04558-1>.
- Tran, H., K. Khoshelham, and A. Kealy. 2019. "Geometric Comparison and Quality Evaluation of 3D Models of Indoor Environments." *ISPRS Journal of Photogrammetry & Remote Sensing* 149:29–39. <https://doi.org/10.1016/j.isprsjprs.2019.01.012>.
- Uddin, M., and M. R. Hassan. 2022. "A Novel Feature Based Algorithm for Soil Type Classification." *Complex & Intelligent Systems* 8 (4): 3377–3393. <https://doi.org/10.1007/s40747-022-00682-0>.
- Van Eck, N. J., and L. Waltman. 2014. "Visualizing Bibliometric Networks." In *Measuring Scholarly Impact: Methods and Practice*, edited by Y. Ding, R. Rousseau, and D. Wolfram, 285–320. Springer, Cham. https://doi.org/10.1007/978-3-319-10377-8_13.
- Yu, Y., T. Xu, Z. Shen, Y. Zhang, and X. Wang. 2019. "Compressive Spectral Imaging System for Soil Classification with Three-Dimensional Convolutional Neural Network." *Optics Express* 27 (16): 23029–23048. <https://doi.org/10.1364/OE.27.023029>.
- Zhang, X., N. H. Younan, and R. L. King. 2003. "Soil Texture Classification Using Wavelet Transform and Maximum Likelihood Approach." Vol. 4. In *IGARSS 2003. 2003 IEEE International Geoscience and Remote Sensing Symposium. Proceedings (IEEE Cat. No.03CH37477)*, Toulouse, France, 2888–2890. IEEE. <https://doi.org/10.1109/IGARSS.2003.1294621>.
- Zhang, X., N. H. Younan, and C. G. O'Hara. 2005. "Wavelet Domain Statistical Hyperspectral Soil Texture Classification." *IEEE Transactions on Geoscience & Remote Sensing* 43 (3): 615–618. <https://doi.org/10.1109/TGRS.2004.841476>.

- Zhang, Y., and A. E. Hartemink. 2019. "Digital Mapping of a Soil Profile." *European Journal of Soil Science* 70 (1): 27–41. <https://doi.org/10.1111/ejss.12699>.
- Zhao, X., Y. Ke, J. Zuo, W. Xiong, and P. Wu. 2020. "Evaluation of Sustainable Transport Research in 2000–2019." *Journal of Cleaner Production* 256:120404. <https://doi.org/10.1016/j.jclepro.2020.120404>.
- Zhao, Y., and C. Teng. 2025. "Classification of Soil Layers in Deep Cement Mixing Using Optimized Random Forest Integrated with AB-SMOTE for Imbalance Data." *Computers and Geotechnics* 179:106976. <https://doi.org/10.1016/j.compgeo.2024.106976>.